

Middle Rio Grande Physical Modeling

Native-topography dataset evaluation summary

S. Michael Scurlock, Christopher I. Thornton, Amanda L. Cox, and Steven R. Abt

Peer Technical Review by Drew C. Baird, Bureau of Reclamation, Denver Technical Service
Center, Denver Colorado

August 2012



Colorado State University
Engineering Research Center
Department of Civil and Environmental Engineering

Middle Rio Grande Physical Modeling

Native-topography dataset evaluation summary

Prepared by:

Colorado State University
Daryl B. Simons Building at the
Engineering Research Center
Fort Collins, Colorado 80523

Prepared for:

U.S. Department of the Interior
Bureau of Reclamation
Albuquerque Area Office
555 Broadway N.E., Suite 100
Albuquerque, New Mexico 87102-2352

This research has been completed at Colorado State University with funding from the U. S. Bureau of Reclamation in Albuquerque, NM, via U. S. Forest Service Contract: 07-JV-221602-264. This research was supported in part by funds provided by the Rocky Mountain Research Station, Forest Service, U. S. Department of Agriculture.

Table of Contents

EXECUTIVE SUMMARY	1
INTRODUCTION.....	2
PLANIMETRIC VELOCITY DISTRIBUTION IN THE PRISMATIC AND NATIVE- TOPOGRAPHY MODELS.....	10
INSTREAM STRUCTURE HYDRAULICS WITHIN THE NATIVE-TOPOGRAPHY MODEL	16
MIDDLE RIO GRANDE PHYSICAL MODEL RESEARCH SUMMARY	23
<i>Sin (2010) and Ursic (2011).....</i>	<i>24</i>
<i>Scurlock et al. (2012b).....</i>	<i>24</i>
<i>Scurlock et al. (2012c).....</i>	<i>25</i>
<i>Scurlock et al. (2012d).....</i>	<i>25</i>
<i>Current research.....</i>	<i>26</i>
MIDDLE RIO GRANDE MODEL RECOMMENDATIONS	26
CONCLUSIONS.....	29
REFERENCES.....	29
APPENDIX.....	33

List of Figures

Figure 1. Middle Rio Grande River prototype area (Walker, 2009)	3
Figure 2. Constructed trapezoidal channel model	4
Figure 3. Trapezoidal model plan view.....	4
Figure 4. Prototype reach topographies	6
Figure 5. Native-topography construction framework and rock fill.....	6
Figure 6. Native-topography plan view schematic and constructed surface.....	7
Figure 7. Plan schematic of parameters in Equation 2.....	9
Figure 8. Profile view schematic of evaluated structures in trapezoidal model.....	9
Figure 9. Channel bend hydraulic schematic, from Ottevanger et al. (2011).....	11
Figure 10. Schematic of trapezoidal model of Heintz (2002).....	12
Figure 11. Data-collection locations of Walker (2009) (<i>left</i>) and Scurlock et al. (2012) (<i>right</i>)	13
Figure 12. 60% flow-depth velocity magnitudes for the trapezoidal model.....	14
Figure 13. Velocity magnitudes as various percentage depth for the native- topography 8 ft ³ /s discharge	15
Figure 14. Velocity magnitudes as various percentage depth for the native- topography 12 ft ³ /s discharge	16
Figure 15. 60% flow-depth velocity magnitudes in the trapezoidal (<i>left</i>) and native-topography (<i>right</i>) models for the trapezoidal maximum reduction design.....	17

Figure 16. 60% flow-depth velocity magnitudes in the trapezoidal (<i>left</i>) and native-topography (<i>right</i>) models for the trapezoidal minimum reduction design.....	18
Figure 17. Observed and predicted <i>MVR</i> and <i>AVR</i> for the native-topography spur-dikes	22

List of Tables

Table 1. Type I and Type III model bend characteristics	5
Table 2. Maximum outer-bank velocity and MVR_O for trapezoidal and native-topography structures	18
Table 3. Regression results for Equation 1 from Scurlock et al. (2012)	20
Table 4. Native-topography spur-dike characteristics.....	20
Table 5. Native-topography observed and predicted velocity ratios	20
Table 6. Native-topography observed and predicted root mean square deviation and mean absolute percent error	21
Table 7A. Summary of contractual items and deliverables.....	33

Executive Summary

Colorado State University initiated a physical modeling program under contract by the United States Bureau of Reclamation in 2001. The purpose of the program was to investigate channel-bend hydraulics and induced transverse instream-structure hydraulics installed for the mitigation of undesired bank erosion. An emphasis was placed on development of transverse feature design procedures. A trapezoidal, prismatic model and a model representing surveyed prototype data were constructed, and velocity and boundary shear-stress data were collected and analyzed. Summary of the conclusive findings from the collected data are provided.

The analyses performed on the trapezoidal and native-topography models led to valuable insights into the nature of channel-bend hydraulics, boundary shear-stress distributions, induced structure hydraulics, and transverse instream structure performance. Collected data from the model were visualized and compared with distributions from the literature. Velocity patterns within the native-topography and trapezoidal models were analyzed. Boundary shear-stress distributions were examined, methodologies for the prediction of longitudinal shear-stress distribution were developed, and current design guidelines were updated. Empirical design equations were developed for the prediction of induced maximum and average hydraulics from transverse instream structures.

Further details and benefits of each analysis component from the physical model of the Middle Rio Grande are identified and limitations are discussed. Limitations are primarily a product of data resolution and constraints of modeled parameters. Further research is proposed to complete the development of design procedures for trapezoidal and naïve-bed topography channels. Suggestions for further data analyses of collected data, collection of supplemental physical model data, and the evaluation of a series of newly constructed physical and numerical models are provided.

Introduction

River environments are complex and dynamic systems wherein localized and regional geologic, geographic, ecologic, meteoric, and anthropogenic influences dictate the characteristics of the flow path and behavior. In 1975, Cochiti Dam was installed in a braiding geomorphic regime of the Middle Rio Grande River upstream of Albuquerque, New Mexico. The braiding system present before installation was typical for the distance of the river along the path from its mountainous headwaters, as well as the localized sediment gradation, slope, and vegetation recruitment. The installation of the Cochiti Dam effectively stores all sediment. In addition past channelization work and levee construction altered the channel. The combined effects have resulted in a geomorphic shift from a braiding to slightly sinuous single thread channel which can migrate laterally placing riverside infrastructure in danger of erosional damage. The Albuquerque Area Office (AAO) of the United States Bureau of Reclamation (Reclamation) as part of its maintenance program has sought to mitigate undesired channel migration within the study reach of the Middle Rio Grande. The AAO identified a variety of transverse instream structures as potential mitigation measures of undesired channel migration within the Middle Rio Grande and contracted Colorado State University (CSU) to conduct a series of physical models to investigate the hydraulic conditions associated with such structures. Quantification of the distribution of boundary shear stress at flow conditions without structures was also emphasized for the evaluation of zones requiring increased protection measures.

A concrete, trapezoidal, 1:12 Froude-scaled physical model was constructed in 2001 at CSU consisting of two representative channel bends of the Middle Rio Grande set in series with a transition zone in between. Figure 1 depicts the Middle Rio Grande prototype reach, Figure 2 provides a photograph of the constructed prismatic model, and Figure 3 provides a schematic of the model planform geometry. Details of the construction process and selection of the prismatic bend geometries are detailed in Heintz (2002). Table 1 provides the characteristics of the trapezoidal channel bends including channel top width, radius of curvature, bend angle, relative curvature, and channel length.

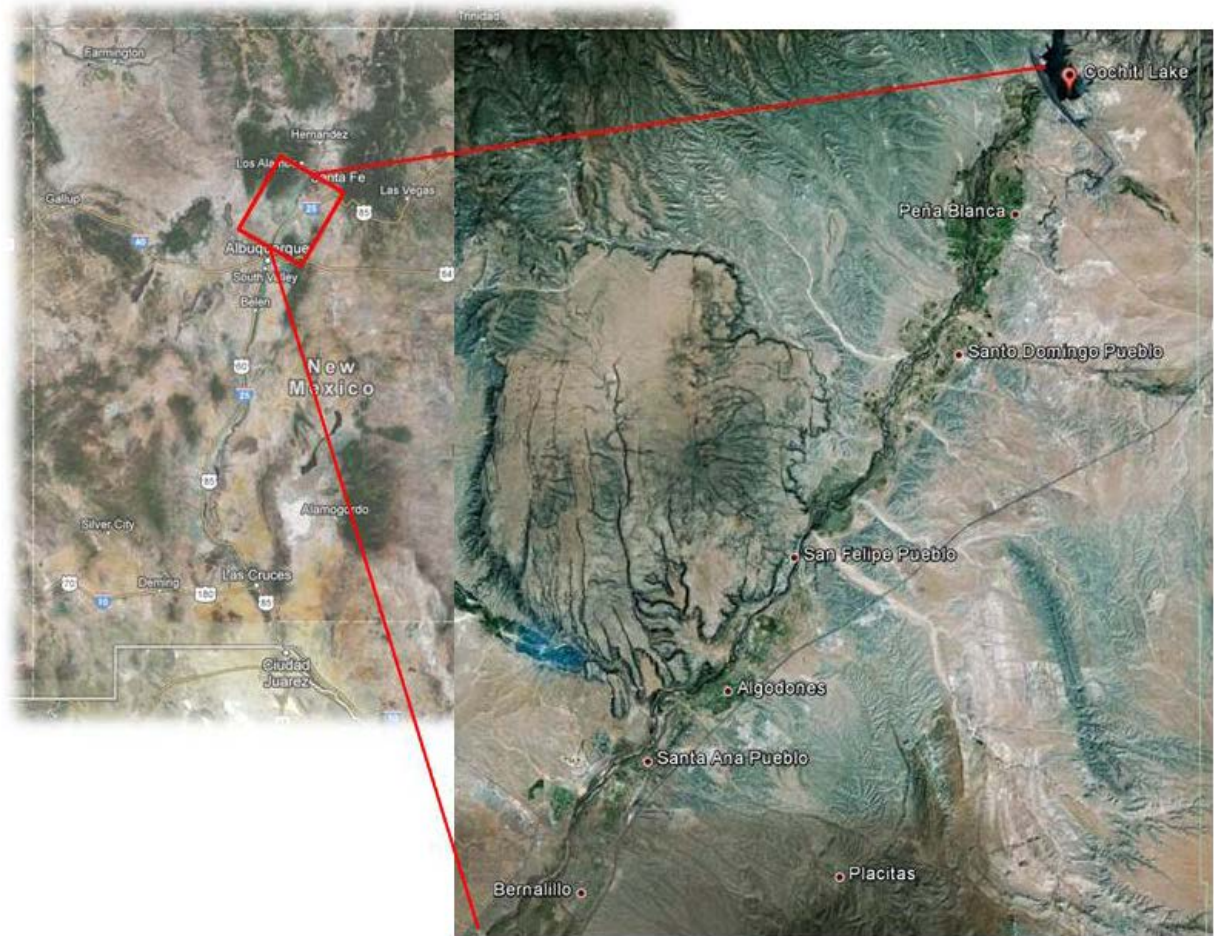


Figure 1. Middle Rio Grande River prototype area (Google, 2012)



Figure 2. Constructed trapezoidal channel model

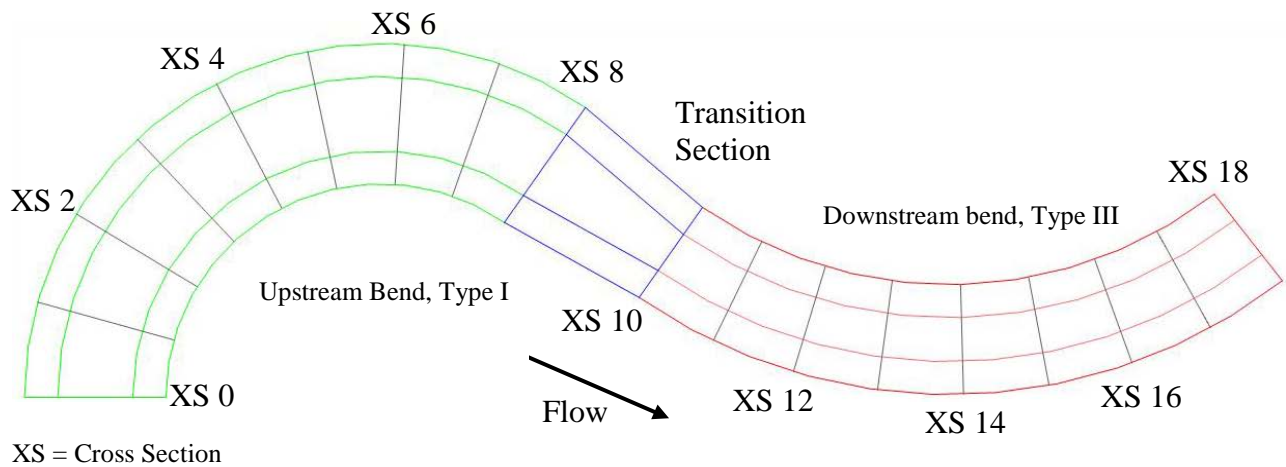


Figure 3. Trapezoidal model plan view

Table 1. Type I and Type III model bend characteristics

Type	Top Width	Radius of Curvature	Bend Angle	Relative Curvature	Channel Length
	<i>ft (m)</i>	<i>ft (m)</i>	<i>(degrees)</i>	R_C/T_W	<i>ft (m)</i>
Type I	19.2 (5.9)	38.75 (11.81)	125	2.02	84.5 (25.8)
Type III	15 (4.6)	65.83 (20.06)	73	4.39	83.5 (25.5)

At the conclusion of the trapezoidal model testing, CSU was contracted to continue physical modeling, expanding the planimetric representation of the prototype reach to encompass channel topographies representative of the Middle Rio Grande. Alteration from the trapezoidal to the native topography allowed for evaluation of the influence of a migrating channel thalweg, pool and run sequencing, and variable transverse slope on channel-bend hydraulics as compared to the prismatic channel.

Survey data were acquired for the Cochiti and San Felipe bends as detailed by Reclamation (2000) from the study reach of the Middle Rio Grande River. The Cochiti bend had similar planimetric channel characteristics as the Type-III trapezoidal bend, and the San Felipe bend resembled the Type-I trapezoidal bend. Ten transverse cross sections, identified as M1 through M10, were extracted from the surveyed data by Reclamation for characterization of geomorphic features for each reach. Figure 4 provides plan views of the selected channel reaches with identified prototype cross sections. Figure 5 illustrates the cross-sectional templates, support cross-sectional framework, and fill material. Figure 6 illustrates a plan-form schematic of the channel and a representation of the model surface interpolated from LIDAR data. Further details of the cross-section scaling, bed material sizing, and other pertinent information regarding the model construction are provided in Walker (2009).

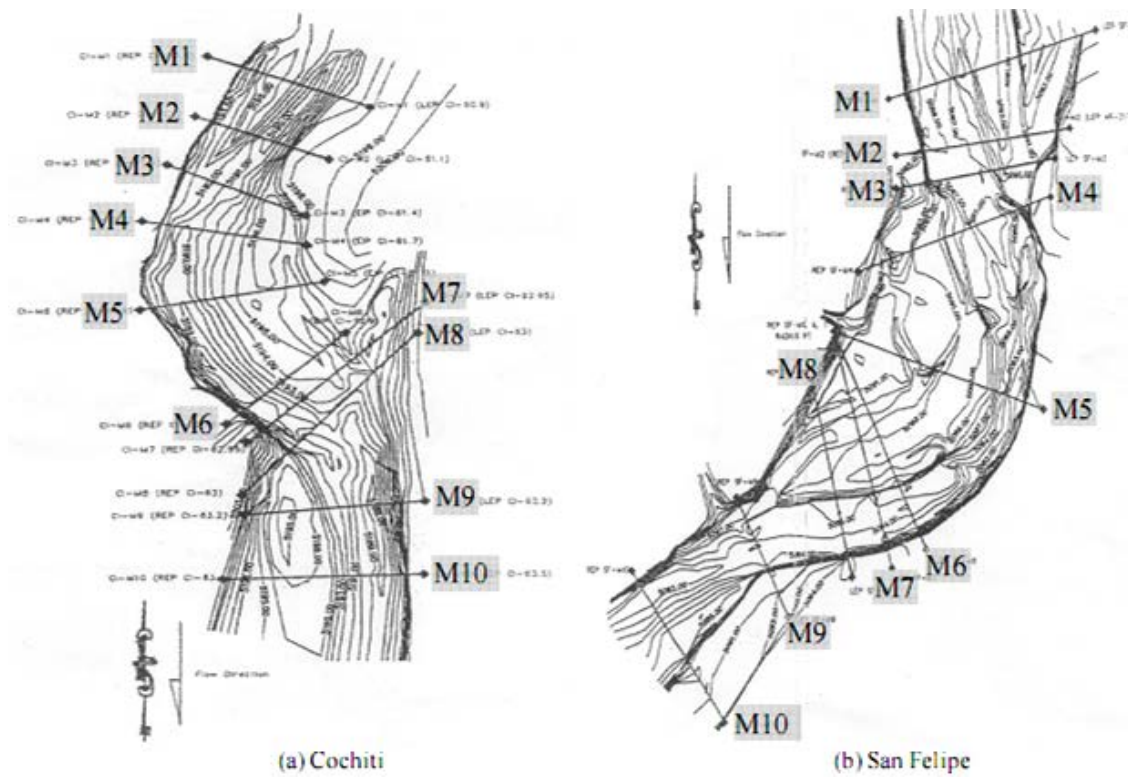


Figure 4. Prototype reach topographies



Figure 5. Native-topography construction framework and rock fill

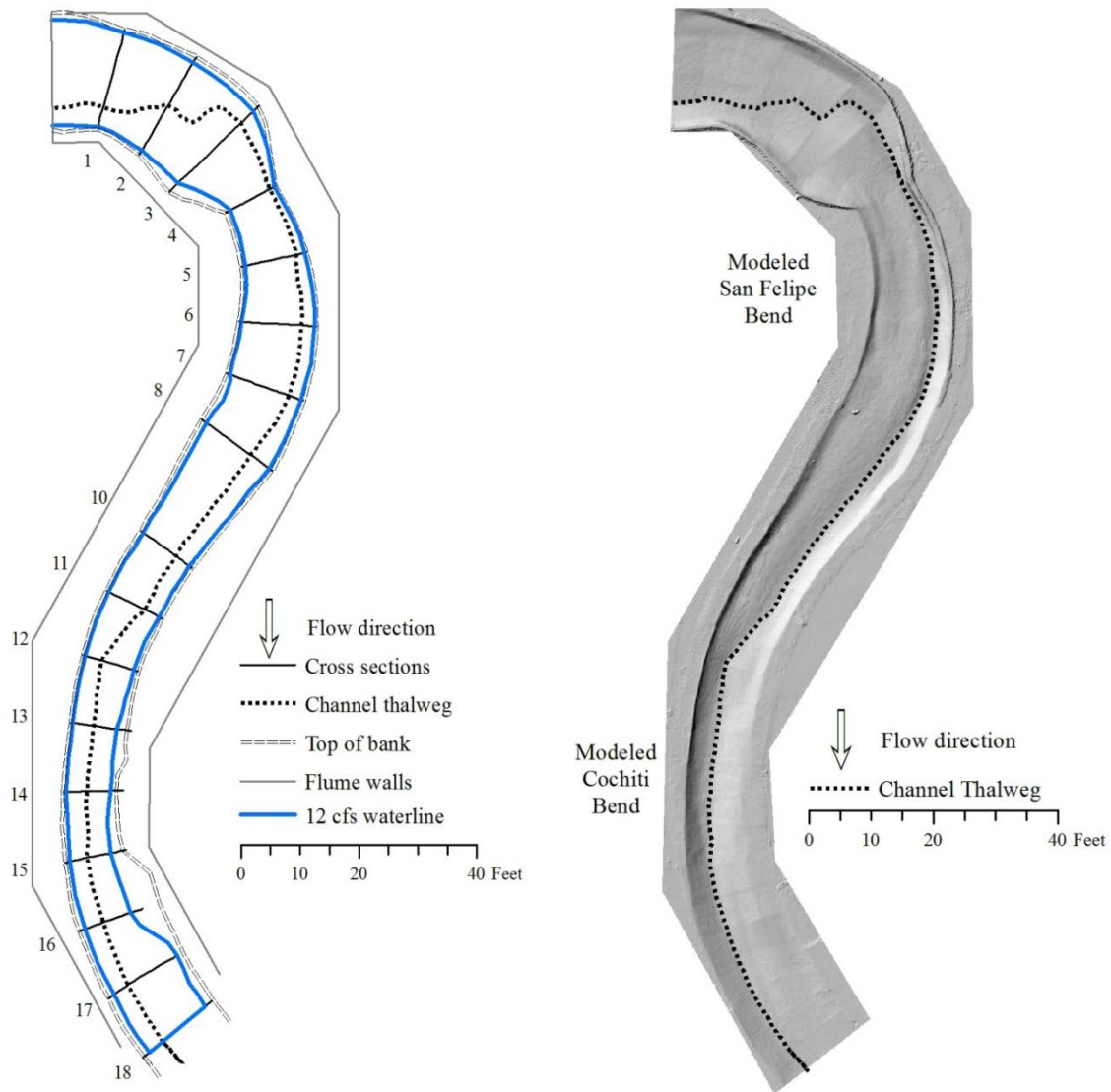


Figure 6. Native-topography plan view schematic and constructed surface

Following the completion of the construction of the trapezoidal and native-topography models, velocity and boundary shear-stress data were collected under a variety of flow conditions. For the trapezoidal model, $8 \text{ ft}^3/\text{s}$, $12 \text{ ft}^3/\text{s}$, $16 \text{ ft}^3/\text{s}$, and $20 \text{ ft}^3/\text{s}$ discharges were evaluated under normal-depth downstream boundary conditions. Heintz (2002) and Sin (2010) detailed the baseline data collection of the trapezoidal model. The native topography was evaluated for $8 \text{ ft}^3/\text{s}$, $12 \text{ ft}^3/\text{s}$, and $16 \text{ ft}^3/\text{s}$ under draw-down downstream boundary conditions as reported by Walker (2009). Normal-depth downstream boundary conditions were evaluated in the native-topography model for $4 \text{ ft}^3/\text{s}$, $8 \text{ ft}^3/\text{s}$, and $12 \text{ ft}^3/\text{s}$ discharges as reported by Scurlock et al. (2012c). A comprehensive report and comparison of all baseline data compiled from the native-topography is reported by Scurlock et al. (2012c). Normal-depth flow is characterized by

equivalent longitudinal gradients of the water-surface elevation, energy-grade line, and bathymetry. The control on the hydraulic conditions within the channel is dictated by the channel geometry and roughness. For draw-down profiles, the water-surface elevation and energy-grade line gradually steepens in the downstream direction towards a hydraulic control less than normal depth. Chow (1959) provides a thorough review of gradually-varied and uniform flow conditions in open channels.

Boundary shear-stress data within the trapezoidal model at baseline conditions were analyzed by Sin (2010), and Urisc (2011) analyzed native-topography data collected under draw-down boundary conditions. Scurlock et al. (2012d) performed a literature review on the distribution of boundary shear stress in channel bends, and used data from both the trapezoidal and native-topography models under all downstream boundary conditions to develop statistically derived design equations for channel-bend stabilization design.

Following the evaluation of baseline flow conditions within the models, sets of transverse instream structures designed for outer-bank velocity and shear stress reduction were installed and induced hydraulic effects were quantified. Three structure types were investigated in the trapezoidal model; spur-dikes and submerged spur-dikes by Heintz (2002) and Darrow (2004), and vanes by Schmidt (2005). Spur-dikes are installed with flat structure crests set at the design-flow elevation (Federal Highway Administration, 2005), vanes typically tie into the bank at the design-flow elevation and have sloping structure crests (Bhuiyan, 2010), and bendway weirs have flat structure crests typically set at one-half or less design flow depth (Federal Highway Administration, 2005; McCullah and Gray, 2005; Julien and Duncan, 2003). Bendway weirs evaluated within the trapezoidal model were noted as high-crested, due to the structure crest height set above the recommended one-half design flow depth. Figure 7 illustrates a planimetric schematic of all transverse instream structures evaluated, and Figure 8 depicts profile views of the spur-dikes, vanes, and submerged spur-dikes as evaluated in the laboratory. Scurlock et al. (2012b) investigated the maximum-velocity ratio (*MVR*), and the average-velocity ratio (*AVR*) within the trapezoidal model and developed a suite of regression equations which describe induced hydraulics as functions of the design parameters.

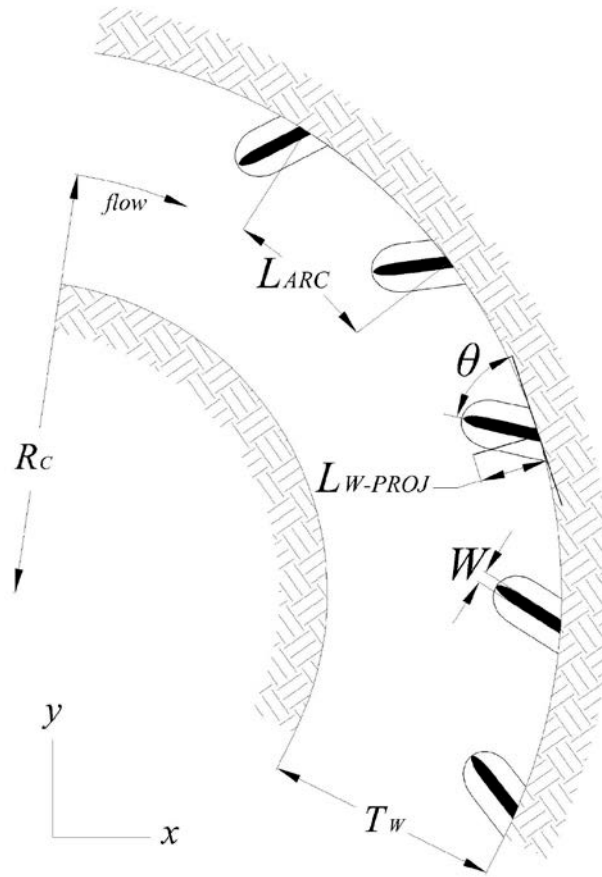


Figure 7. Plan schematic of parameters in Equation 2

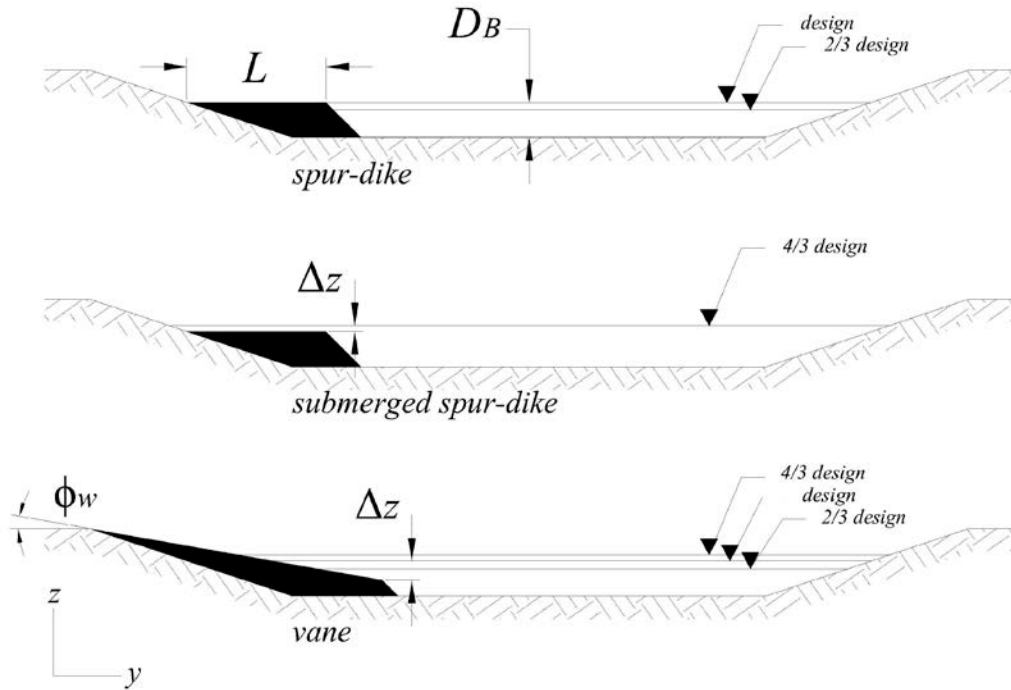


Figure 8. Profile view schematic of evaluated structures in trapezoidal model

Two configurations were identified from the trapezoidal model exhibiting the maximum and minimum velocity reduction from baseline conditions. The maximum reduction was found in the upstream, Type-I bend and the minimum was found in the downstream, Type-III bend. The structures were selected for installation in the native-topography model to bracket the range of induced velocity effects, and the maximum and minimum design was installed in both Type-I and Type-III bends. Identified spur-dike structures were the installed in the native-topography with the same spacing, angle, and percentage cross-sectional area blocked as the trapezoidal configurations. Youngblood et al. (2011) detailed the structure selection, construction methods, and collected data from the structure installations in the native-topography model.

The physical-model representations of the Middle Rio Grande study reach have been the source of substantial data acquisition in order to facilitate a variety of goals. The purposes of this paper are to compare the velocity distributions of the trapezoidal and native-topography models, to compare the maximum and minimum structure designs between the trapezoidal and native-topography models, to summarize the various research objectives and findings of the project, and to provide recommendations for future research objectives to fulfill the goals of the project. Two analyses are performed unique to this research: baseline velocity trends recorded within the trapezoidal and native-topography models are presented and trends are comparatively analyzed; and the empirical relationships for the prediction of *MVR* and *AVR* from Scurlock et al. (2012b) are applied to the native-topography structures from Youngblood et al. (2011). Other research performed in the prismatic and native-topography model is summarized with major findings and recommendations presented. Further testing and data evaluation recommendations are presented which draw from collected data and performed analyses in order to facilitate a comprehensive and definitive conclusion to the project goals.

Planimetric velocity distribution in the prismatic and native-topography models

Velocity distributions within an open-channel stream bend are complex and three-dimensional; yet have exhibited characteristic, recurring trends as reported from the literature. Channel-bend flow velocity patterns arise from centrifugal forces acting on the flow and differential pressure across the channel due to water surface super-elevation along the outside of the channel bend. Figure 9 presents a schematic of open-channel river-bend flow. Transverse circulation associated with the main secondary current combined with longitudinal velocity results in helical flow paths through the channel bend. A smaller, tertiary counter-rotating cell is present near the water surface at the outside of the channel bend. The flow velocity evolves throughout the channel bend, with the highest velocity magnitudes beginning on the inside bank, then transitioning to the outer bank through the bend. Kalkwijk and de Vriend (1980) and Blanckaert and de Vriend (2003 and 2004), Blanckaert and Graf (2001), Ottevanger et al. (2011), and Julien (2002) describe river-bend flow velocity characteristics.

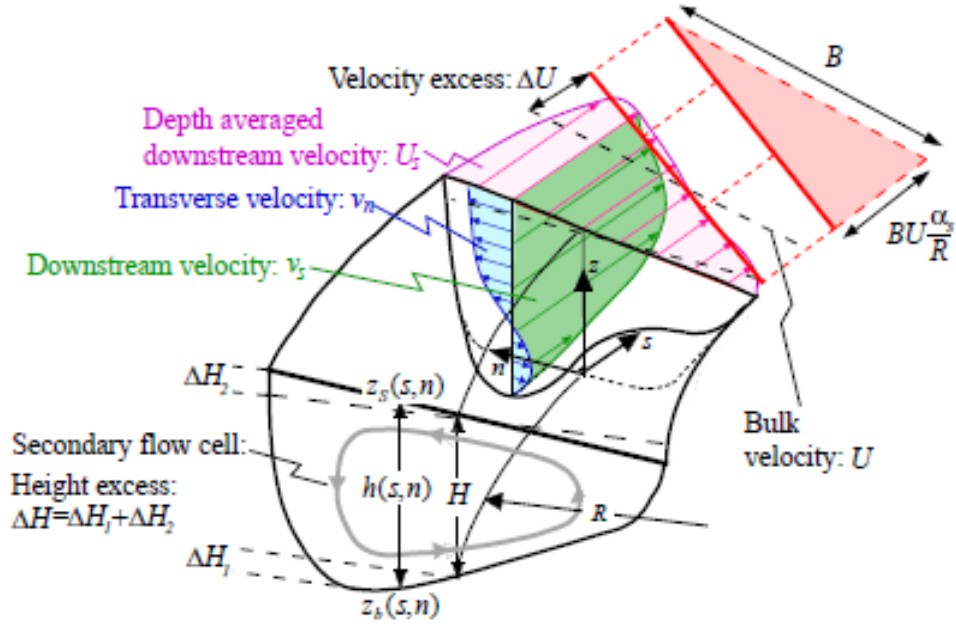


Figure 9. Channel bend hydraulic schematic, from Ottevanger et al. (2011)

Planimetric distributions of depth-averaged velocity magnitudes have been shown by Pacheco-Ceballos (1983) to follow the boundary shear-stress within a channel bend. Scurlock et al. (2012d) demonstrated that the most common areas of high shear stress in channel bends occur at the inner-bank at the bend entrance, and the outer-bank at the bend exit, with a trending increase in shear stress along the outer-bank and decrease in shear-stress along the inner-bank. Velocity data were obtained with an acoustic Doppler velocimeter (ADV) for the trapezoidal model as detailed by Heintz (2002) and for the native-topography model as detailed by Walker (2009) and Scurlock et al. (2012c). Figure 10 illustrates the planimetric velocity data-collection locations in the trapezoidal model. Vertical distribution of the planimetric velocity data-collection locations are further detailed by Heintz (2002). Figure 11 provides the velocity data-collection locations within the native-topography model for the draw-down and normal-depth boundary conditions. Further details regarding the vertical velocity profiles taken for each boundary condition are provided by Walker (2009) and Scurlock et al. (2012c). The trapezoidal boundary conditions were uniformly set at normal-depth across all flow rates. The present analysis focuses on the comparisons between the planimetric depth-averaged velocity distributions for the trapezoidal and native-topography models.

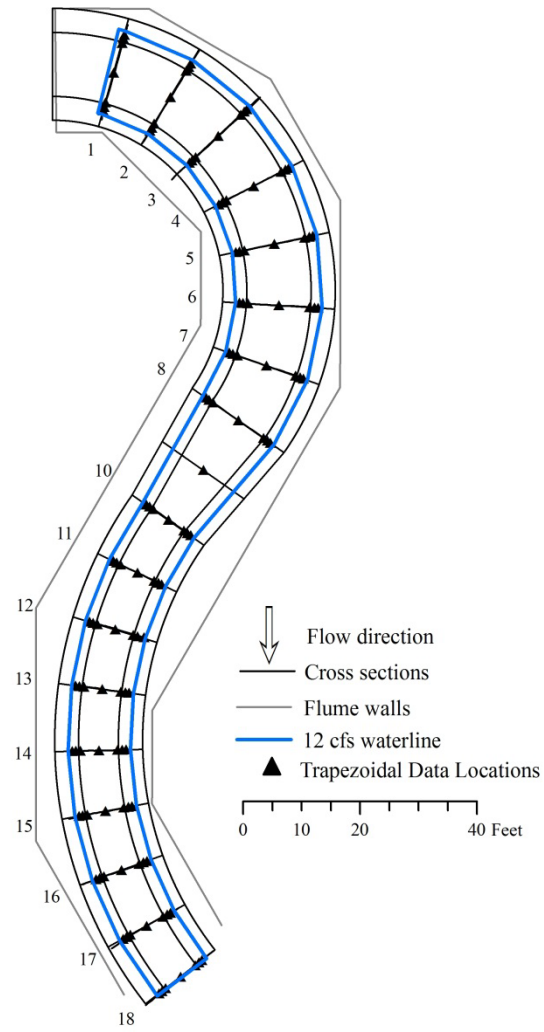


Figure 10. Schematic of trapezoidal model of Heintz (2002)

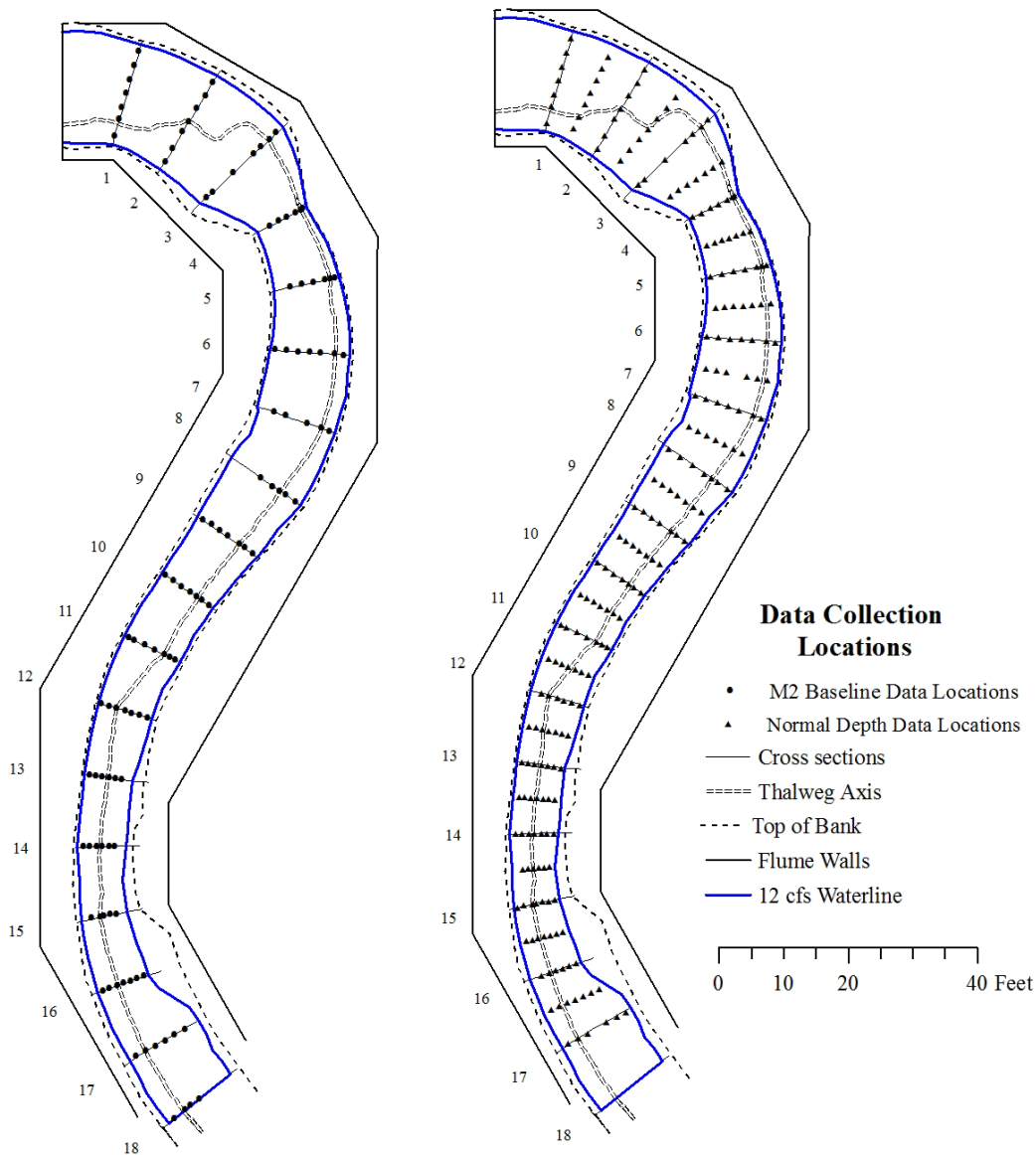


Figure 11. Data-collection locations of Walker (2009) (*left*) and Scurlock et al. (2012c) (*right*)

Time-averaged velocity magnitudes taken at 60% flow-depth below the water-surface elevation were utilized as an approximation to the depth-averaged velocity magnitudes. Data are reported by Heintz (2002) and Scurlock et al. (2012c). Data were interpolated to the extent of the wetted perimeter using a spline technique truncated to the maximum, or below the minimum recorded. Figure 12 illustrates the interpolated velocity results from the trapezoidal model for all evaluated discharges. For the upstream Type-I bend, the trapezoidal model exhibited a zone of higher velocity along the inner-bank at the bend entrance which gradually shifted to the outer-bank at the bend exit. After the bend apex, the inner-bank velocity was relatively low compared to the outer-bank velocity, which corresponds well to point-bar formation zones from the literature. For the downstream, Type-III bend, the high velocity core also migrated from the inner-bank at the bend entrance to the outer-bank at the bend exit. Slower velocities were

observed at the inner bank after the bend apex. For both channel bends, the highest velocities measured were not found at the outer-bank, but proximal to the outer-bank toe and at the inner-bank entrance. Blanckaert and Graf (2004) indicated that the zone of highest outer-bank shear stress does not occur on the channel bank, but at the inner edge of the outer-bank boundary. Data collection within the trapezoidal model were sparse, and little information regarding flow patterns in the center of the channels was obtained. The flow patterns roughly adhere to expected trends from the high shear-stress zones observed from the literature and Scurlock et al. (2012d).

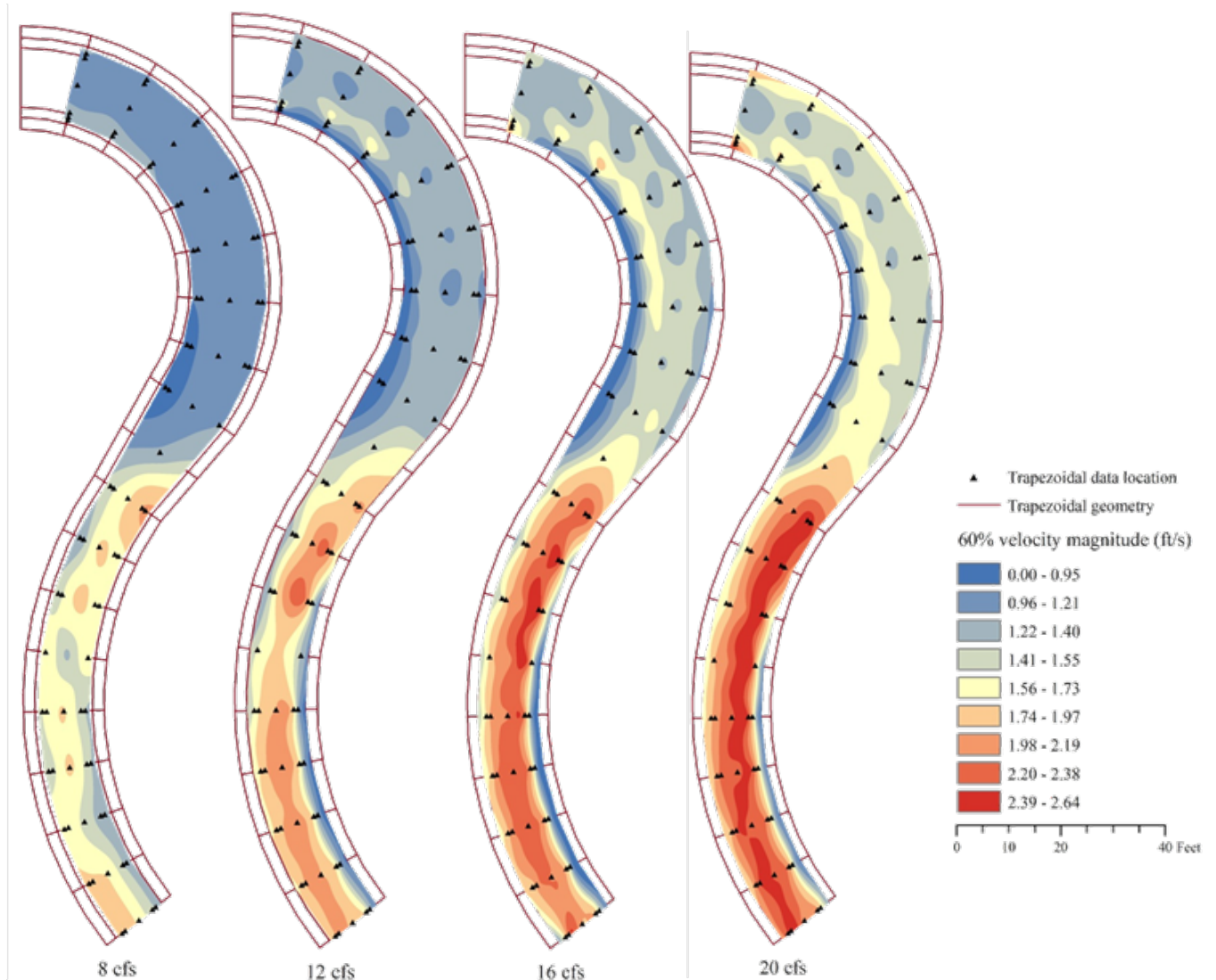


Figure 12. 60% flow-depth velocity magnitudes for the trapezoidal model

The 8 ft³/s and 12 ft³/s discharges were the only two flow rates evaluated in both the trapezoidal and native-topography models under similar downstream boundary conditions. Figure 13 and Figure 14 present the interpolated velocity magnitudes collected within the native-topography model for 8 ft³/s and 12 ft³/s discharges, respectively. Scurlock et al. (2012c)

detailed the velocity distributions of the other discharges and boundary conditions evaluated within the native-topography model. Similar trends are depicted in the native-topography as were observed with the trapezoidal model. Zones of high velocity were typically found at the bend entrance at the inner-bank, and the bend exit at the outer-bank. At 60% flow depth, the maximum velocities at the outer-bank were not located at the wetted-perimeter extents, but were approximately centered over the channel thalweg, corresponding to the trapezoidal results and tertiary current bank-protection theory of Blanckaert and Graf (2004). The native topography contained rigid-bed contractions which influenced the flow conditions, including a planimetric choke, a vertical contraction due to a thalweg migration, and a high point-bar area in the Type-I bend, and another vertical contraction due to thalweg migration in the Type III bend. Native-topography channel-bed features resulted in higher variability of flow patterns; however, general trends coinciding with the literature are still apparent.

Compared with the trapezoidal model, the velocity distributions within the native-topography are larger in magnitude. The maximum values for the native-topography velocities at 60% flow-depth at normal-depth downstream conditions are 0.783 ft/s and 0.160 ft/s higher than the trapezoidal model for the 8 ft³/s and 12 ft³/s discharges. The channel top-width, flow area, and roughness values changed between the trapezoidal and native-topography models; and therefore, direct quantitative comparison between the two physical models is not feasible.

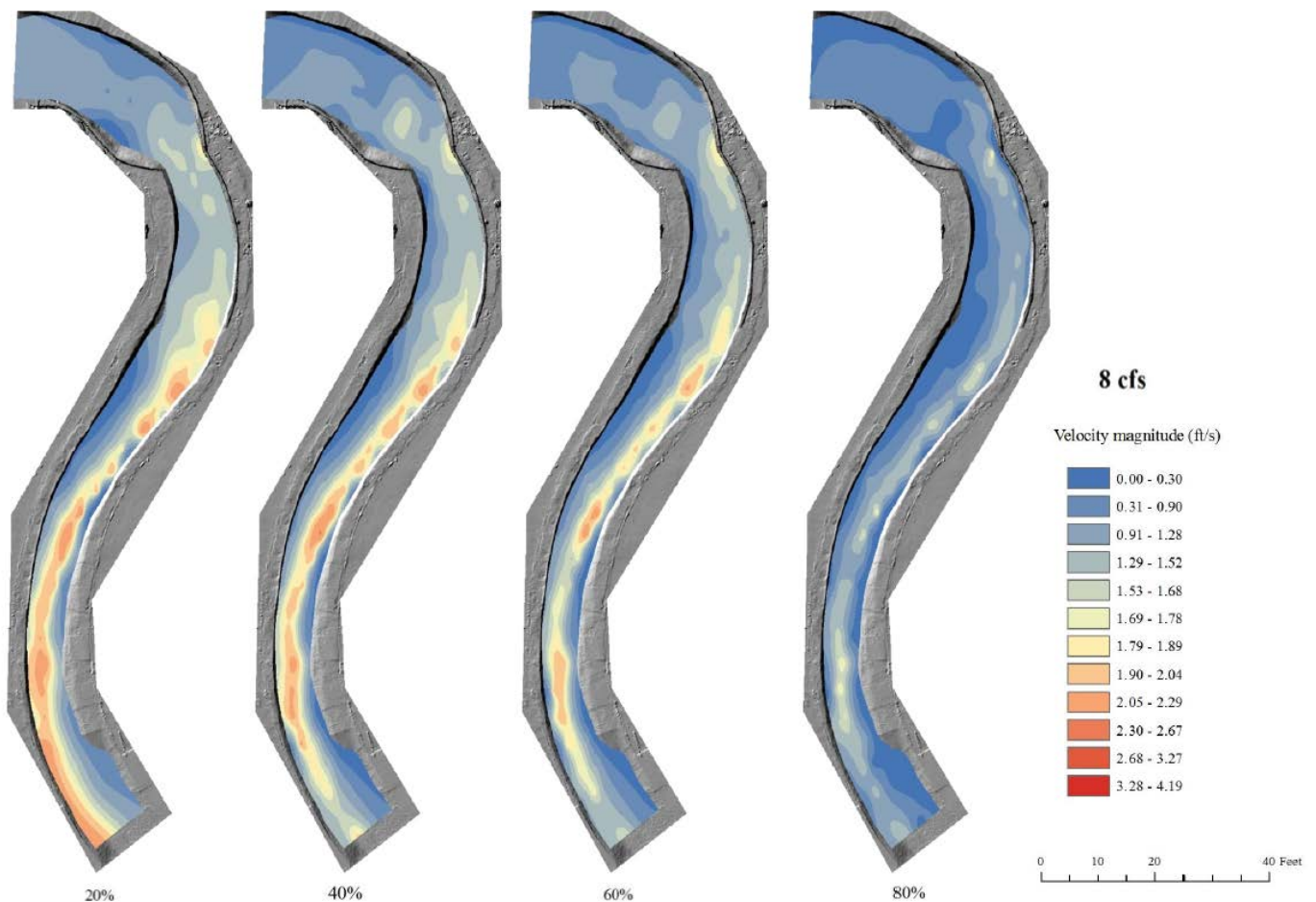


Figure 13. Velocity magnitudes as various percentage depth for the native-topography 8 ft³/s discharge

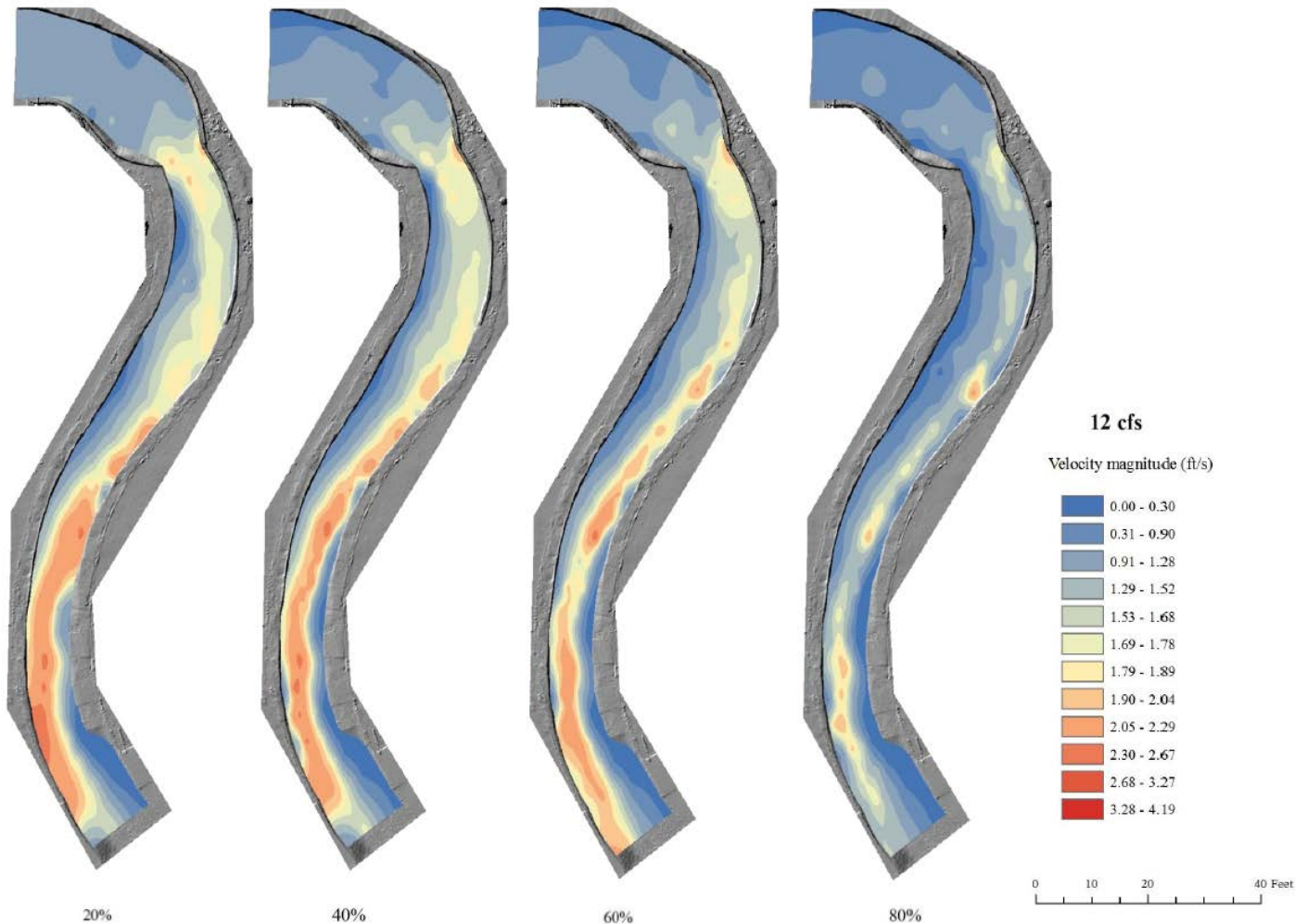


Figure 14. Velocity magnitudes as various percentage depth for the native-topography 12 ft³/s discharge

Transverse instream structure hydraulics within the native-topography model

Heintz (2002), Darrow (2004), and Schmidt (2005) constructed and evaluated 130 independent transverse instream structure configurations in the trapezoidal model, comprised of 60 spur-dikes, 40 vanes, and 30 submerged spur-dikes. Youngblood et al. (2011) installed the maximum and minimum velocity reduction design from the trapezoidal configurations in the native-topography model. Figure 15 depicts interpolated velocity data for the maximum configuration from the trapezoidal model compared with the maximum configuration in the same bend of the native-topography model, and Figure 16 depicts the minimum configurations. Table 2 presents the maximum outer-bank velocity and MVR_O for the native-topography and trapezoidal spur-dikes. Nomenclature of configurations was adapted from Heintz (2002) and Youngblood et al. (2011), with TW04 and TW10 corresponding to the minimum and maximum trapezoidal configurations, and NW01 through NW04 corresponding to the native-topography configurations. The observed velocities within the native topography spur-dikes were over 1.0 ft/s higher for the maximum and minimum designs than the trapezoidal model. The trapezoidal MVR_O was less than one for the minimum and maximum configurations, and were less than the

native-topography ratios for all configurations. Spatial gradients in the velocity magnitudes observed within the maximum configuration were more substantial for the native-topography structures than for the trapezoidal. While the maximum velocity within the native-topography structure field displayed values greater than the trapezoidal model, the area adjacent to the outer-bank in the native-topography maximum-reduction spur-dike field exhibited velocities on the same order as the trapezoidal model. For the minimum configuration, the spur-dike installation in the native-topography failed to reduce high velocities after the fifth weir, as numbered sequentially in the downstream direction. The zone of maximum velocity with the structures coincides with the baseline-condition location for the native-topography. For the minimum configuration in the native-topography model, velocities higher than baseline were recorded within the spur-dike field, represented by *MVR* values greater than one.

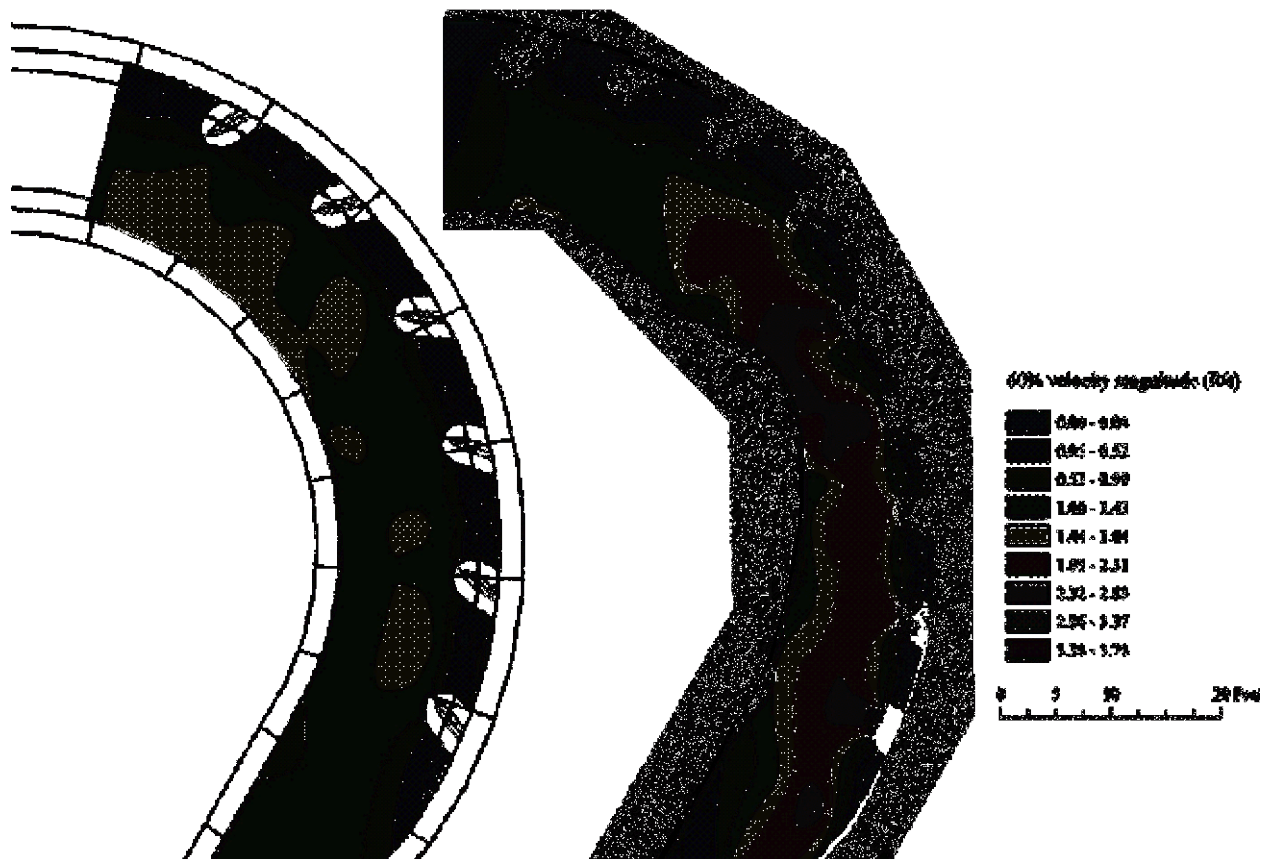


Figure 15. 60% flow-depth velocity magnitudes in the trapezoidal (*left*) and native-topography (*right*) models for the trapezoidal maximum reduction design

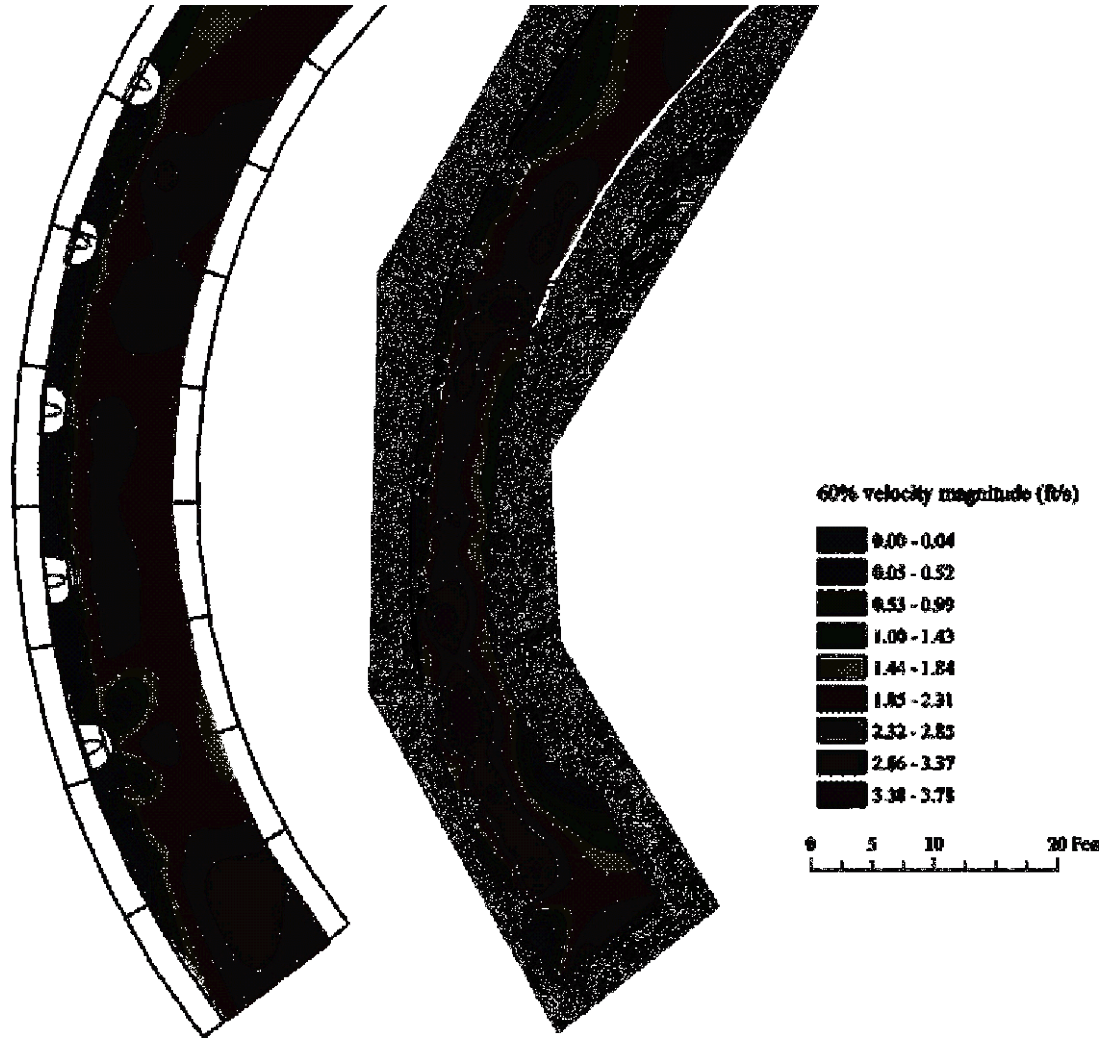


Figure 16. 60% flow-depth velocity magnitudes in the trapezoidal (*left*) and native-topography (*right*) models for the trapezoidal minimum reduction design

Table 2. Maximum outer-bank velocity and MVR_O for trapezoidal and native-topography structures

Configuration	Maximum outer-bank velocity ft/s	Observed MVR_O
-	-	-
NW01 (<i>minimum</i>) Type III	3.542	1.410
NW02 (<i>maximum</i>) Type I	1.223	0.715
NW03 (<i>maximum</i>) Type III	1.630	0.649
NW04 (<i>minimum</i>) Type I	2.926	1.711
TW04 Type III(NW04, NW01)	1.672	0.906
TW10 Type I(NW03, NW02)	0.155	0.255

Scurlock et al. (2012) developed a suite of empirical design equations to estimate the maximum-velocity ratio and bend-average velocity ratio at different locations in the channel bend from the trapezoidal dataset. The generalized regression model of Scurlock et al. (2012b) is presented as Equation 1.

$$MVR, AVR = a_1 (A^*)^{a_2} \left(\frac{L_{ARC}}{T_W} \right)^{a_3} \left(\frac{R_C}{T_W} \right)^{a_4} \left(\frac{L_{W-PROJ}}{T_W} \right)^{a_5} \left(\frac{D_B}{D_B - \Delta z} \right)^{a_6} \left(\frac{2\theta}{\pi} \right)^{a_7} \quad (1)$$

where:

A^* = percentage of projected cross-sectional weir area to baseline cross-sectional flow area at design flow;

L_{W-PROJ} = projected length of structure into channel [L];

L_{ARC} = arc length between centerline of structures [L];

R_C = radius of curvature of channel bend [L];

T_W = averaged top width of channel measured at baseline in bend [L];

D_B = averaged maximum cross-section baseline flow depth in bend [L];

Δz = elevation difference between water surface and structure crest [L];

θ = structure plan angle [radians]; and

a_1, \dots, a_6 = regression coefficients.

The regression coefficients of Equation 1 were specific to structure type, and the inner-bank, centerline, and outer-bank channel locations. Table 3 details the coefficients determined by Scurlock et al. (2012b) for all structures and isolated, spur-dike data. Equation 1 was applied to data collected from the native-topography spur-dike configurations. Non-prismatic channels exhibit varying top-widths, flow depths, and cross-sectional flow areas as opposed to approximately static values for prismatic channels. Reach-averaged parameters were used in the implementation of Equation 1 for the native-topography model. The regression equations for all structure types and for the spur-dike structures from Scurlock et al. (2012b) were applied to the current dataset. Table 4 provides the terms of Equation 1 from the native-topography spur dikes.

The R_C/T_W term in the Type III bend, corresponding to NW01 and NW03, was outside of the limits of the parameter ranges used for regression analyses on Equation 1. The reach-averaged ratio of R_C/T_W for the Type III native-topography bend was calculated at 8.151, while the maximum limit for the trapezoidal model was 6.862. Table 5 details the results of the application of Equation 1 to the native-topography spur-dikes and Table 6 summaries the root mean square deviation (RMSD) and mean absolute percent error (MAPE) between the observed and predicted results of Equation 1 applied to the native-topography spur-dikes. Figure 17 presents the observed and predicted MVR and AVR for both equations. For the outer-bank velocity ratios, the observed values are the most significantly under-predicted of all results. The centerline maximum ratio is under predicted and the averaged ratio does not display trends. The inner-bank ratios do not display trends for the all-structure data equation, and is under-predicted for the spur-dike equation. For the minimum configurations, the mean absolute percent error was approximately 56%, and for the maximum configurations, the mean absolute percent error was approximately 36% for the equation generated for all the trapezoidal structure types. The mean absolute percent error was approximately 115% for the minimum configurations, and was approximately 80% for the maximum configurations for the spur-dike specific equation.

Table 3. Regression results for Equation 1 from Scurlock et al. (2012)

All Data (130)	R^2	$MA\%E$	a_1	a_2	a_3	a_4	a_5	a_6	a_7
<i>MVRo</i>	0.8429	20.8533	0.0068	0.0000	0.5546	0.3846	-2.1431	0.7003	0.3824
<i>MVRc</i>	0.8011	4.3100	0.3773	0.2695	0.0000	0.1973	-0.1563	0.0467	0.1155
<i>MVRi</i>	0.6087	4.4433	0.3400	0.3404	-0.1116	0.1065	-0.2084	0.0445	0.1580
<i>AVRo</i>	0.4861	40.7230	0.0138	0.0000	0.5917	0.7439	-1.1451	0.4629	0.5996
<i>AVRc</i>	0.7255	4.0327	0.3615	0.2710	-0.0739	0.1850	-0.1412	0.0536	0.1158
<i>AVRi</i>	0.7530	3.9452	0.1315	0.4894	-0.1308	0.1770	-0.4098	0.1170	0.1266

Spur dike (60)	R^2	$MA\%E$	a_1	a_2	a_3	a_4	a_5	a_6	a_7
<i>MVRo</i>	0.8317	20.7074	5.648E-11	3.5354	1.1335	0.0000	-7.8000	-1.9823	0.5963
<i>MVRc</i>	0.9014	3.2235	1.7160	0.0000	-0.0881	0.2674	0.3711	0.1581	0.1970
<i>MVRi</i>	0.6215	4.9464	2.1970	0.0000	-0.0434	0.0000	0.2684	0.2087	0.2253
<i>AVRo</i>	0.7305	28.5942	4.175E-11	3.5645	1.0828	0.0000	-7.5607	-2.1849	0.0000
<i>AVRc</i>	0.7914	3.3918	1.7267	0.0000	-0.1023	0.1758	0.3473	0.1971	0.2053
<i>AVRi</i>	0.7876	3.6910	1.9293	0.0000	-0.1468	0.1512	0.3831	0.4048	0.1835

Table 4. Native-topography spur-dike characteristics

Configuration	Bend	R_C	T_W	L_{ARC}	L_{WPROJ}	θ	A^*
-	-	ft	ft	ft	ft	degrees	-
NW01	Type III	72.900	8.943	14.040	1.735	90	19.506
NW02	Type I	47.116	13.035	13.310	3.759	60	10.784
NW03	Type III	72.900	8.943	13.310	2.663	60	10.753
NW04	Type I	47.116	13.035	14.040	2.224	90	19.392

Table 5. Native-topography observed and predicted velocity ratios

Configuration	Velocity ratio (VR)	Baseline Velocity	Max/Avg Velocity	Observed VR	Predicted VR	Abs. % error: all-structure equation	Predicted spur-dike VR	Abs. % error: spur-dike equation
-	-	ft/s	ft/s	-	-	-	-	%
NW01 (Minimum trapezoidal)	<i>MVRo</i>	2.512	3.542	1.410	0.658	62.075	5.197E-09	184.368
	<i>MVRc</i>	2.512	3.328	1.325	1.642	27.885	1.103	2.188
	<i>MVRi</i>	2.512	3.035	1.208	1.564	34.253	2.468	91.399
	<i>AVRo</i>	2.512	2.255	0.898	0.561	43.575	0.000	137.478
	<i>AVRc</i>	2.512	2.675	1.065	1.453	42.466	1.262	23.818
	<i>AVRi</i>	2.512	2.385	0.949	1.506	68.224	1.310	32.805
NW02 (Maximum trapezoidal)	<i>MVRo</i>	1.711	1.223	0.715	0.139	112.827	8.028E-10	367.867
	<i>MVRc</i>	1.711	3.078	1.799	1.070	56.779	1.146	13.034
	<i>MVRi</i>	1.711	2.611	1.526	1.062	42.559	2.155	100.252
	<i>AVRo</i>	1.711	0.463	0.271	0.118	78.836	4.385E-10	163.466
	<i>AVRc</i>	1.711	2.226	1.301	0.992	33.282	1.254	32.755
	<i>AVRi</i>	1.711	1.590	0.930	0.834	14.454	1.240	69.068
NW03 (Maximum trapezoidal)	<i>MVRo</i>	2.512	1.630	0.649	0.218	77.167	9.613E-09	255.447
	<i>MVRc</i>	2.512	3.926	1.563	1.248	23.390	1.160	14.693
	<i>MVRi</i>	2.512	3.491	1.390	1.102	24.082	2.268	97.372
	<i>AVRo</i>	2.512	0.649	0.258	0.261	1.253	4.051E-09	85.057

Configuration	Velocity ratio (VR)	Baseline Velocity <i>ft/s</i>	Max/Avg Velocity <i>ft/s</i>	Observed VR	Predicted VR	Abs. % error: all-structure equation	Predicted spur-dike VR	Abs. % error: spur-dike equation %
-	-	-	-	-	-	-	-	-
	<i>AVRc</i>	2.512	2.651	1.055	1.115	6.608	1.256	31.246
	<i>AVRi</i>	2.512	2.971	1.183	0.903	27.480	1.186	18.769
NW04	<i>MVRo</i>	1.711	2.926	1.711	0.514	97.960	4.341E-10	237.811
(<i>Minimum trapezoidal</i>)	<i>MVRc</i>	1.711	3.451	2.017	1.425	41.108	1.062	26.617
	<i>MVRi</i>	1.711	2.231	1.304	1.533	24.615	2.345	92.186
	<i>AVRo</i>	1.711	1.436	0.839	0.284	92.612	2.187E-10	210.979
	<i>AVRc</i>	1.711	2.359	1.379	1.307	7.303	1.239	19.413
	<i>AVRi</i>	1.711	1.594	0.932	1.440	76.343	1.349	47.496

Table 6. Native-topography observed and predicted root mean square deviation and mean absolute percent error

Configuration	RMSD	Spur-dike equation RMSD	MAPE	Spur-dike equation MAPE
NW01 (<i>minimum</i>)	0.477	0.876	46.413	78.676
NW02 (<i>maximum</i>)	0.449	0.501	56.456	124.407
NW03 (<i>maximum</i>)	0.273	0.493	26.664	83.764
NW04 (<i>minimum</i>)	0.633	0.985	56.657	105.750

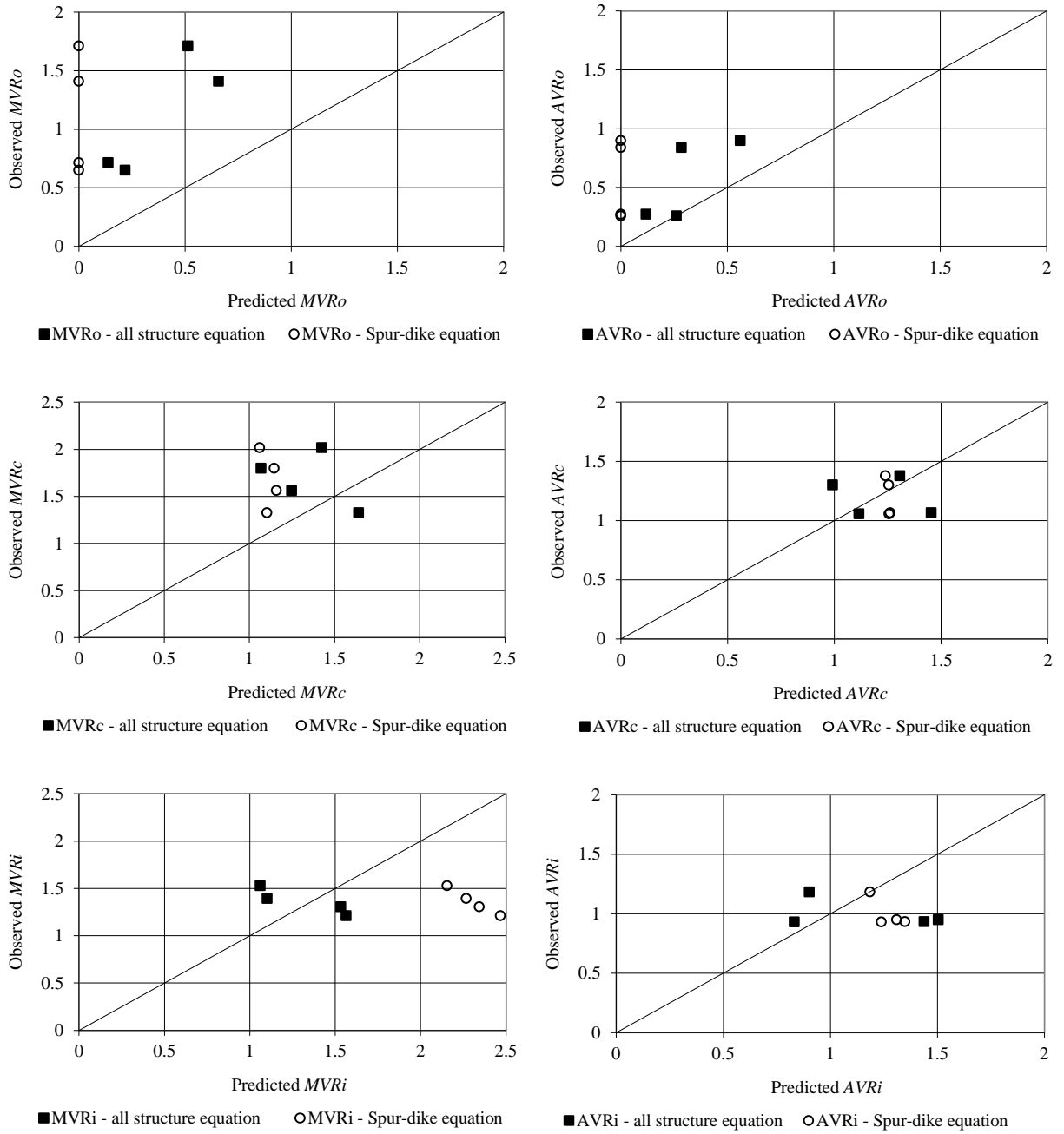


Figure 17. Observed and predicted MVR and AVR for the native-topography spur-dikes

Results indicate that equations developed by Scurlock et al. (2012b), and the reach-averaged parameter technique, may not directly apply to non-prismatic channels. An offset equation or the development of equations tailored to native topographies may be required for such channels. Construction methods used in the development of the native-topography spur-dikes kept the cross-sectional area the same across the reach. Varying top-width and cross-sectional flow area in the native topography resulted in necessary variance of the length of the weir crest at each location to keep A^* consistent within the channel bend. Therefore, at each

weir, the parameters of Equation 1 are unique, and calculated values for MVR and AVR change along the channel path. An assumption of channel-bend averaged parameters was implemented in the evaluation of Equation 1. Error in prediction may have been a result of such assumptions.

Marginal applicability of the trapezoidal model velocity-ratio equations may also be a result of the rigid-bed topography of the native channel and the construction methods used for the installation of the weirs. It was observed that installation of the minimum-reduction configuration in the native-topography increased the outer-bank velocities, with MVR_O values of 1.71 and 1.41 for the Type I and Type III bends, respectively. Maximum-reduction configurations reduced velocity, with MVR_O values of 0.72 and 0.65 for the Type I and Type III bends, respectively, yet were reduced much less than the trapezoidal installation which had a MVR_O value of 0.255. Maintaining cross-sectional area blocked within each structure configuration, instead of another parameter such as structure crest length, may have adversely affected applicability of the equations. The rigid, natural bed of the native-topography contained planimetric and vertical contractions. The native bathymetry may have induced localized hydraulics which skewed the values of MVR and AVR from the relatively uniform condition of the trapezoidal model, either through inciting bend-flows associated with natural channel-bend topography or through localized contraction hydraulics. Scurlock et al. (2012d) demonstrated that localized gradients in the native-topography surface significantly affected the distributions of shear stress.

The empirical equations of Scurlock et al. (2012b) are limited to specific, and somewhat constrictive, parameter ranges evaluated in the trapezoidal model. It was determined that the averaged R_C/T_W value for the Type III bend exceeded the ranges of trapezoidal data used for the development of regression coefficients. Coefficients of determination for Equation 1 as provided in Table 3 range from 0.4 to 0.9. Error in the prediction of the native-topography MVR and AVR are therefore affected by the inherent prediction error of the equations.

Four spur-dike configurations installed in native-topography after the trapezoidal minimum and maximum outer-bank velocity reduction configurations were evaluated with the design equations of Scurlock et al. (2012b). Equation 1 was tailored to the data collected from the trapezoidal model with regression analyses on parameter coefficients. It was shown that application of Equation 1 to native-topography spur-dikes produced reasonable values, but mean absolute error approached 56% for the all-structure equations and 124% for the spur-dike specific equations. Prediction error was hypothesized to be a result of reach-averaged parameter calculations, construction methods of the native topography and structures, or the variance in the prediction accuracy of Equation 1 of the trapezoidal data.

Middle Rio Grande physical model research summary

Findings from research conducted on the native topography dataset illuminated valuable insights to the nature of channel-bend flow patterns, and to induced transverse instream structure hydraulics. Scurlock et al. (2012b) expanded on results from Scurlock et al. (2012a) and investigated effects on velocity from spur-dike, vane, and submerged spur-dike installations in the trapezoidal model, incorporating the results of Heintz (2002), Darrow (2004), and Schmidt (2005). Walker (2009) and Scurlock et al. (2012c) presented velocity and boundary shear-stress data collected from the native-topography model. Sin (2010) and Ursic (2011) analyzed methodologies of determining the boundary shear-stress within respective trapezoidal and native-

topography models. Scurlock et al. (2012) investigated the planimetric and longitudinal distribution of boundary shear stress within the trapezoidal and native-topography models. The current research depicted planimetric trends and comparisons between the trapezoidal and native-topography physical models and applied results of Scurlock et al. (2012b) to the native-topography transverse instream structures. Research performed on previously collected data has provided valuable information representing breakthroughs in the engineering community; however, limitations of application of results and findings to field design scenarios have been identified. Fundamental findings and limitations from the seminal reports of Sin (2010), Ursic (2011), Scurlock et al. (2012b), Scurlock et al. (2012c), and Scurlock et al. (2012d) describing the Middle Rio Grande physical project objectives are described.

Sin (2010) and Ursic (2011)

Trapezoidal and native-topography shear-stress data prediction methodologies were examined by Sin (2010) and Ursic (2011). Both authors proposed design criteria based off the observed maximum normalized shear-stress in the respective models. Sin (2010) evaluated the methods of one-dimensional momentum equation, Rozovskii (1961), Reynolds stress, log-law, and Preston-tube shear-stress estimates in the trapezoidal model. Ursic (2011) compared the one-dimensional momentum equation, turbulent kinetic energy, Reynolds stress, log-law, and Preston-tube shear-stress estimates within the native-topography model. Both authors concluded that the Preston-tube was the most accurate method of direct measurement of shear stress at the boundary, and they found that the readings were higher than other methods, providing more conservative results. Sin (2010) stated that the limitations of the study were the ranges of discharges evaluated, and the flow-depth limitations of the ADV used for data collection. Ursic (2011) noted that the shape of the native-topography bed surface had a large influence on the distribution of shear-stress and recommended incorporating a factor to account for the variable bathymetry for shear-stress prediction. Ursic (2011) further recommended adjustment of the proportionality constant in the turbulent kinetic energy shear-stress prediction method to better represent meandering stream flows.

Scurlock et al. (2012b)

The ratio of the maximum velocity and bend-averaged velocity found at the inner-bank, centerline, and outer-bank of a trapezoidal channel bend with installed instream structures was investigated by Scurlock et al. (2012b). Research conducted was founded in data collected, and conclusions drawn, by Heintz (2002), Darrow (2004), and Schmidt (2005). The prediction method of Equation 1 was proposed, and regression procedures were performed to create a suite of empirical design tools. Scurlock et al. (2012b) noted that the equations are limited to the bounds of the data used for regression parameter determination, and that extrapolation results in uncertain prediction error. Authors note that the maximum velocity ratio is dependent upon capturing the global maximum point velocity value within the channel bend, which is a function of data resolution. Results of Scurlock (2012a) were incorporated in the work of Scurlock et al. (2012b), which indicated that there may be a limit of A^* and R_C/T_W where the regression equations break down. Recommendations for identifying this limit, and to make the

methodologies more robust included the expansion of the dataset for empirical regression. It was concluded that a numerical model be implemented to investigate a wide variety of structure types and configurations installed in various channel-bend geometries under different flow conditions. The model would be validated with collected physical model data, then expanded to provide new, high-resolution data for instream structure hydraulics.

Scurlock et al. (2012c)

Velocity and shear-stress patterns within the native-topography channel were provided for baseline draw-down and normal-depth downstream boundary conditions by Scurlock et al. (2012c). Effects of contractions in the native-topography bed surface were found to significantly affect velocity and boundary shear-stress distributions. Collected velocity data were used to show the conveyance shift and secondary current development in the channel bends. Collected velocity data for the normal-depth boundary conditions is of sufficient resolution to perform further analyses to supplement gaps in the literature. Authors recommend evaluation of the momentum and vorticity equations along the course of the flow through the channel bend to aid in illumination of important characteristic hydraulics. Spatiotemporal turbulence analysis of the flume data was recommended as a means of better understanding the channel bend velocity and shear-stress distributions. To substantially increase the amount of data at a fraction of the physical modeling cost, a numerical model validated with physical data was recommended for further evaluation of the dataset. The numerical model may also be used to incorporate additional prototype locations to the analysis using field survey data. It was hypothesized that the native-topography channel would reconfigure if it possessed a non-rigid bed surface. A live-bed model was recommended for evaluation of equilibrium hydraulics in the channel bends.

Scurlock et al. (2012d)

Boundary shear-stress calculation methodologies were reviewed and the planimetric and longitudinal distributions within the trapezoidal and native-topography models at baseline conditions were analyzed. The design equations from Sin (2010) and Ursic (2011) were revised. Design recommendations for the shear-stress evolution through the course of natural channels were proposed. Morphologic indicators were examined for the prediction of boundary shear-stress along the flow path. It was concluded that the data resolution in the trapezoidal model did not capture the dominant boundary shear-stress zones within the channels. High shear-stress zones in the native-topography were adequately captured, but the effects of the rigid native-topography bed, especially in the Type I bend, significantly affected shear-stress distributions. It was recommended that a numerical model be implemented to investigate the boundary shear-stress distribution in the trapezoidal model. Numerical modeling would expand the range of discharges, bathymetric shapes, planimetric geometries, and roughness characteristics to make design methodologies substantially more robust. A live-bed model was recommended for further evaluation of natural-channel hydraulics which would naturally adjust to areas of high boundary shear stress.

Current research

The evaluation of velocity magnitudes and distributions for the baseline and instream-structure configurations of the trapezoidal and native-topography models illuminated key findings. Baseline velocity patterns roughly adhered to the zones of high shear stress as indicated by Scurlock et al. (2012d). Velocities distributions were similar for both models, yet magnitudes were different as a result of change in flow area and roughness characteristics. The data resolution within the baseline trapezoidal channel was sparse, and velocity trends may not have been fully realized. The native-topography velocity distributions were affected by the rigid-bed vertical and planimetric contractions in the bathymetry.

The planimetric distribution of velocity in the native-topography spur-dikes was compared to the trapezoidal configurations. For the minimum configuration in the native-topography model, velocities higher than baseline were recorded, represented by *MVR* values exceeding one. Findings indicate that transverse instream structure installation in a channel bend may increase outer-bank erosion if improperly sized.

Velocity ratio equations of Scurlock et al. (2012b) were applied to the native-topography spur-dikes. It was found that while the equations generally gave reasonable values, the percentage error ranged from 27% to 124%. It was hypothesized that the cumulative error was a result of intrinsic error associated within the design equations, the construction methods of the native-topography model and structures, or the reach-averaged parameter calculation method used in the implementation of the equations. Recommendations from this research included increasing the data resolution in the trapezoidal baseline model and examination of additional instream-structure configurations with the use of a numerical model.

Middle Rio Grande model recommendations

The culmination of data collection and analyses for the Middle Rio Grande modeling project has resulted in important findings and a clear path for further testing in order to realize the main goals of the project. A summary of the documents detailed in this report, along with other associated analyses are presented in the Appendix. The main recommendations for further testing arise from the poor data resolution and parameter variability, and from the implications of rigid-bed natural topography. The implementation of a numerical model for all studies in which the boundary is immobile is recommended. Physical modeling of instream-structure stability is recommended in a mobile-bed setting. Further analyses on the collected data are recommended which could be further expanded by physical and numerical modeling.

Advances in computation technology and numerical models of fluid flow have made the prospect of accurate simulation of channel-bend hydraulics a reality. Examples of application of a numerical model to the case of channel-bend flows are given by Constantinescu et al. (2011), Shams et al. (2002), Wu et al. (2000), Zeng et al. (2008), and Khosronejad et al. (2007). Commercial codes, such as FLOW-3D, have been used successfully in the past for open-channel bend flows with in-stream structures (Abad et al., 2008). Government software, such as U²RANS, has been used successfully by Holmquist-Johnson (2011) and others to investigate complex, three-dimensional open-channel flow environments. Data resolution in a numerical model is on the order of the numerical grid used for calculation, and would be much finer than that collected in the physical model. Data from the Middle Rio Grande model would be used to validate the numerical model. Physical model limitations are such that changing the radius of

curvature, slope, roughness, or bathymetry in a channel bend is economically and temporally demanding. Numerical modeling is not limited in this regard, and alteration of such parameters is relatively quick and simple. As such, a calibrated numerical model could vastly expand the current dataset in a fraction of the time already invested in the project. The main benefits of a numerical model, and the scope of numerical-model research would entail the following:

- Expand the trapezoidal, instream-structure dataset to include higher parameter variability in the evaluated configurations. Currently, design methodologies are limited to two values of R_C/T_W , three values of A^* , two values of θ , and small ranges of spacing and structure length. Regression-based design equations are limited by these data ranges. Expansion of the ranges through numerical modeling of various structure parameter configurations, in a wide range of R_C/T_W channels, would vastly improve the prediction methodologies. Prismatic geometries are easily generated in a numerical model. The near-continuous nature of data resolution from a numerical model would ensure that the true maximum velocity and boundary shear-stress were measured within the structure configuration.
- Investigate instream structure configurations within the native-topography model. Four spur-dikes were evaluated in the native topography model, and they were shown to exhibit hydraulic characteristics different than trapezoidal configurations of similar geometry. A numerical representation of the native-topography is easily achievable from high-precision LIDAR topographic data from the physical model. Altering the parameters of the instream structures evaluated in the physical model would provide further insight to the behavior of instream-structure hydraulics in natural channel bends.
- Incorporate surveyed data from other bends in the Middle Rio Grande study reach, and evaluate various structure configurations within numerical representations of the channel bends. The native-topography model contained two prototype bends only, such that adjusting design methodologies for these two bends may not apply to the full spectrum of natural channels. Increasing the number of prototype channels bends for numerical evaluation of instream structure configurations would allow for confident estimation of the regression coefficients of Equation 1 for the study reach.
- Velocity and boundary shear-stress distributions would be available for each numerical simulation. The longitudinal shear-stress distributions and morphologic indicators from Scurlock et al. (2012d) would be greatly improved with the inclusion of data from more channel bends. Numerical modeling would allow for a more confident estimation of the evolution of shear stress along prismatic and natural channel bends, as well as a better prediction of normalized maximum shear-stress in the channel. For the trapezoidal model, the sparse data resolution would be amended with the addition of numerical data.

Numerical models perform well with rigid boundaries; however, deformable-bed models are more computationally intensive and have not yet gained wide acceptance in the engineering community. Instream structures installed in mobile-bed environments incite erosion and sedimentation patterns which can affect structure performance and stability. As shown by Haltigin et al. (2007) and Bhuiyan et al. (2009), the main zones of scour occur in the vicinity of the structure tip as a result of local acceleration and conveyance shift. When flow overtops the structure, as in the case of a bendway weir, the flow accelerates over the weir crest and at the bank-tie in point. Structural stability guidelines and critical failure points and mechanisms can not be fully realized with a numerical model.

It is recommended that the design approaches for rock sizing for instream structures be reviewed and a physical modeling program be initiated for the development of comprehensive design guidance. Physical models should be mobile bed for documentation of the scour progression and depth, and to best describe equilibrium hydraulic conditions as found in field installations. Evaluation of single structures and structures in arrays with mobile bed would be valuable. If the current model was to be modified for the evaluation of equilibrium bed conditions, it is recommended that the native-topography be removed and the trapezoidal model be modified to contain a mobile bed. Development of design equations for rock size, maximum boundary shear-stress and velocity at the structure tip, crest, and tie-in location, and equilibrium scour characteristics is recommended from the physical-model data.

Data collected from the rigid-bed trapezoidal and native-topography models may serve as a first approximation to the proposed design equations for the instream structures with equilibrium mobile-bed conditions. It is recommended that further analyses be conducted on the three structure types in the trapezoidal and native-topography models to quantify the velocity and shear-stress distributions over and around the structures. Findings would serve as important standalone design recommendations, and coupled with the further physical modeling data, would be valuable for installation guidance.

Collected baseline data from the native-topography model is of high quality and resolution, and insight into the character of channel-bend hydraulics may be gained with further data analyses. Application and expansion of methods reported by Blanckaert and Graf (1999), Blanckaert and Graf (2001), Blanckaert and Graf (2004), Blanckaert and de Vriend (2002), Blanckaert and de Vriend (2005), Ottevanger et al. (2011), Sukhodolov et al. (1998), Anwar (1986), Esfahani and Keshavarzi (2011), Zeng et al. (2008), Odgaard and Bergs (1988), Dietrich et al. (1979), and Constantinescu et al. (2011), amongst others, with the collected native topography dataset would be a valuable asset to the scientific community. Evaluation of the governing hydraulic equations, specifically the full momentum and vorticity equations, using collected data would allow for quantification of specific flow phenomenon, such as the secondary current, and its effects on the flow field. Identification of recirculation zones and secondary and tertiary currents in channel bends is important for a more robust understanding of bend hydraulics, and necessary to properly understand effects of transverse instream structure installation. Spatiotemporal turbulence analyses would illuminate length and time scales of micro and macro-scale velocity fluctuation, and may aid in the prediction of shear-stress distributions as a function of both mean turbulent flow. Turbulence characteristics within a channel bend may be important for sediment transport (Anwar, 1987; Jamieson, 2011), habitat characteristics (Tritico, 2009), and in-stream structure integrity.

The combination of further data analyses on the collected dataset from the trapezoidal and native-topography models, physical investigation of rock-sizing guidelines for transverse instream structures, evaluation of erosion and sedimentation patterns and hydraulic effects in a physical model, development of guidelines quantifying flow hydraulics around and over transverse instream structures, and the development of a comprehensive numerical modeling test program would further aid in realizing the goals of the Middle Rio Grande River modeling project. Completion of the recommended research tasks would provide design engineers comprehensive tools for river bends and transverse instream structures. All recommendations for further research have the potential to be conducted at a fraction of the cost and time already invested in the project.

Conclusions

The Middle Rio Grande River physical modeling program was initiated by Reclamation in 2001 and has generated a wealth of data and insight to the nature of channel-bend hydraulics and transverse instream structure performance. Laboratory measurements and performed analyses from the onset of the program until the completion of the native-topography spur-dike evaluations represent breakthroughs in the realm of channel-bend engineering. Velocity and shear-stress data were collected within a prismatic, trapezoidal model and a native-topography model. Models were representative of prototype channel bends. Evaluation of boundary shear-stress at a variety of flow conditions was performed for both models. Transverse instream structures were installed and induced hydraulics were quantified. Design equations were developed for the prediction of spur-dike, vane, and submerged spur-dike induced maximum and average velocities at the inner-bank, centerline, and outer-bank of the trapezoidal channel bend. Equations were applied to structures installed in the native-topography model and results were analyzed.

Recommendations for the full realization of project goals were identified and presented. Numerical modeling was emphasized for future testing in rigid-bed boundaries due to increased data resolution and resource reduction. Mobile-bed physical modeling of transverse instream structures for quantification of scour patterns, failure mechanisms, and structure stability design was proposed as numerical models are not yet reliable for sedimentation dynamics. Further analysis of laboratory measurements to quantify the velocity and shear-stress distributions around the structures was proposed, which could then be expanded with the mobile-bed physical modeling. Additional analyses of previously collected data would aid in the expansion of the body of knowledge regarding channel-bend hydraulics, and could substantially benefit the scientific and engineering community.

Recommended further research is intended to bring the project to a definitive conclusion and provide complete guidelines for transverse instream structure installation for mitigation of outer-bank erosion. The research goals of the Middle Rio Grande River modeling project have implications which would benefit the global scientific and engineering community. Completion of the project to fruition serves the interest of any hydraulic engineer faced with bank erosion mitigation and has the potential to minimize expenditures resulting from structural failure and undesired, induced hydraulics.

References

- Abad, D.A., Rhoads, B.L., Günerlap, ?, Garcia, M.H. (2008). "Flow structure at different stages in a meander-bend with bendway weirs." *J. Hydraul. Engr.*, 134(8), 1052-1063.
- Anwar, H. (1986). "Turbulent structure in a river bend." *J. Hydral. Engr.*, 112(8), 657-669.
- Bhuiyan, F., Hey, R.D., and Wormleaton, P.R. (2009). "Effects of vanes and w-weir on sediment transport in meandering channels." *J. Hydraul. Engr.* 135(5). 339-349.
- Bhuiyan, F., Hey, R.D., and Wormleaton, P.R. (2010). "Bank-attached vanes for bank erosion control and restoration of river meanders." *J. Hydraul. Engr.* 136(9). 583-596.
- Blanckaert, K., and de Vriend, H. (2003). "Nonlinear modeling of mean flow redistribution in curved open channels." *Water Resources Res.*, 39(12), 1375-1389.
- Blanckaert, K., and de Vriend, H. (2004). "Secondary flow in sharp open-channel bends." *J. Fluid Mech.*, 498, 353-380.

- Blanckaert, K., and de Vriend, H. (2005). "Turbulence characteristics in sharp open-channel bends." *Physics of Fluids*. 17.
- Blanckaert, K., and Graf, W.H., (1999). "Outer-bank cell of secondary circulation and boundary shear stress in open-channel bends." *River, Coastal, and Estuarine Morphodynamics*, 1, 1-10.
- Blanckaert, K., and Graf, W.H., (2001). "Mean flow and turbulence in open-channel bend." *J. Hydraul. Engr.*, 127(10), 835-847.
- Blanckaert, K., and Graf, W.H., (2004). "Momentum transport in sharp open-channel bends." *J. Hydraul. Engr.*, 130(3), 186-198.
- Constantinescu, G., Koken, M., and Zeng, J. (2011). "The structure of turbulent flow in an open channel bend of strong curvature with deformed bed: Insight provided by detached eddy simulation." *Water Resources Research*. 47, 1-17.
- Darrow, J.D. (2004). "Effects of bendway weir characteristics on resulting flow conditions." M. S. Thesis. Colorado State University, Department of Civil Engineering. Fort Collins, Colorado.
- Dietrich, W.E., Smith, D.J., and Dunne, T. (1979). "Flow and sediment transport in a sand bedded meander." *J. Geology*, 87(3), 305-315.
- Esfahani, F.S., and Keshavarzi, A. (2011). "Effect of different meander curvatures on spatial variation of coherent turbulent flow structure inside ingoing multi-bend river meanders." *Stoch. Environ. Res. Risk Asses.*, 25, 913-928.
- Federal Highway Administration (2009). "Design of Roadside Channels with Flexible Linings." HEC-15, Federal Highway Administration, September.
- Haltigin, T.W., Biron, P.M., and Lapointe M.F. (2007). "Predicting equilibrium scour hole geometry near angled stream deflectors using a three-dimensional numerical flow model." *J. Hydraul. Engr.* 133(8): 983-988.
- Heintz, M.L. (2002). "Investigation of bendway weir spacing." M. S. Thesis. Colorado State University, Department of Civil Engineering. Fort Collins, Colorado.
- Holmquist-Johnson, C.L. (2011). "Numerical analysis of river spanning U-weirs: Evaluating effects of structure geometry on local hydraulics." Ph.D. Dissertation. Colorado State University, Department of Civil Engineering. Fort Collins, Colorado.
- Jamieson, E.C. (2011). "The role of vorticity, turbulence, and three-dimensional flow structure on the development of scour." Ph.D. Dissertation. University of Ottawa, Department of Engineering. Ottawa, ON, Canada.
- Julien, P.Y. (2002). *River Mechanics*. Cambridge University Press. New York, NY.
- Julien, Pierre, Y. and Duncan, Josh R. 2003. "Optimal design criteria of bendway weirs from numerical simulations and physical model studies." Colorado State University, Department of Civil Engineering, Fort Collins, CO.
- Kalkwijk, J.P.T., and de Vriend, H. J. (1980). "Computation of the flow in shallow river bends." *J. Hydraul. Res.*, 18(4), 327-342.
- Khosronejad, A., Rennie, C.D., Neyshabouri, S.S.A.A., and Townsend, R.D. (2007). "3D numerical modeling of flow and sediment transport in laboratory channel bends." *J. Hydraul. Engr.*, 133(10), 1123-1134.
- McCullah, J.A. and Gray, D., 2005, "Environmentally Sensitive Channel- and Bank-Protection Measures," *NCHRP Report 544*, Transportation Research Board, National Academies of Science, Washington, D.C.

- Odgaard, J.A., and Bergs, M.A. (1988). "Flow processes in a curved alluvial channel." *Water Resources Res.*, 24(1), 45-56.
- Ottevanger, K., Blanckaert, K., Uijttewaalt, W.S.J (2011). "Processes governing the flow redistribution in sharp river bends." *Geomorphology*.
- Pacheco-Ceballos, R. (1983). "Energy losses and shear stresses in channel bends." *J. Hydraul. Engr.*, 109(6), 881-896.
- Rozovskii, I.L. (1961). "Flow of water in bends of open channels." Academy of Sciences of the Ukrainian SSR, Kiev.
- Schmidt, P.G. (2005). "Effects of bendway weir field geometry characteristics on channel flow conditions." M. S. Thesis. Colorado State University, Department of Civil Engineering. Fort Collins, Colorado.
- Scurlock, S.M., Baird, D.C., Thornton, C.I., Abt, S R., and Cox, A L. (2012b). "Middle Rio Grande physical modeling - Transverse instream structure analysis: Maximum and average velocity ratios within the prismatic channel." Colorado State University, Department of Civil Engineering. Fort Collins, CO.
- Scurlock, S.M., Baird, D.C., Thornton, C.I., Abt, S.R., Cobb, A.H., and Cox, A.L. (2012d). "Middle Rio Grande physical modeling - Shear stress distributions within the prismatic and native-topography channels." Colorado State University, Department of Civil Engineering. Fort Collins, CO.
- Scurlock, S.M., Cox, A.L., Baird, D.C., Thornton, C.I., and Abt, S.R. (2012a). "Middle Rio Grande physical modeling - Transverse instream structure analysis: Maximum outer-bank velocity reduction within the prismatic channel." Colorado State University, Department of Civil Engineering. Fort Collins, CO.
- Scurlock, S.M., Cox, A.L., Baird, D.C., Thornton, C.I., Parker, T.R., and Abt, S.R. (2012c). "Middle Rio Grande Physical Modeling - Native topography: Construction and evaluation of baseline hydraulic conditions." Colorado State University, Department of Civil Engineering, Fort Collins, CO.
- Shams, M., Ahmadi, G., and Smith, D.H. (2002). "Computational modeling of flow and sediment transport and deposition in meandering rivers." *Adv. Water Res.*, 25, 689-699.
- Sin, K. (2010). "Methodology for calculating shear stress in a meandering channel." M. S. Thesis. Colorado State University, Department of Civil Engineering. Fort Collins, Colorado.
- Source: "Middle Rio Grande River." 35°26'39.79" N and 106°27'50.93" W. Google Earth. May 4th, 2012. July 25th, 2012.
- Sukhodolov, A., Thiele, M., and Bungartz, H. (1998). "Turbulence structure in a river reach with sand bed." *Water Resources Res.*, 34(5), 1317-1334.
- Thornton, C.I., Cox, A.L, Ursic, M.E., and Youngblood, N.A. (2011). "Data report for completed bendway-weir configurations within the native topography model." Colorado State University, Department of Civil Engineering. Fort Collins, CO.
- Tritico, H. (2009). "The effects of turbulence on habitat selection and swimming kinematics of fishes." Ph.D. Dissertation. University of Michigan, Department of Civil and Environmental Engineering and Natural Resources and Environment. Ann Arbor, MI.
- United States Bureau of Reclamation (2000). "Meander bend surveys, geomorphic data analysis & field data collection report July 1999 through January 2000." U.S. Department of the Interior, Bureau of Reclamation. Albuquerque, NM.

- Urisc, M.E. (2011). "Quantification of shear stress in a meandering native topographic channel using a physical hydraulic model." M. S. Thesis. Colorado State University, Department of Civil Engineering. Fort Collins, Colorado.
- Walker, K.G. (2009). "Comparison of a generalized trapezoidal model to a native topography patterned bed surface model of the Rio Grande." M. S. technical report. Colorado State University, Department of Civil Engineering. Fort Collins, CO.
- Wu, W., Rodi, W., and Wenka, T. (2000). "3D numerical modeling of flow and sediment transport in open channels." *J. Hydraul. Engr.* 126(1), 4-15.
- Zeng, J., Constantinescu, G., and Weber, L. (2008). "A 3D non-hydrostatic model to predict flow and sediment transport in loose-bed channel bends." *J. Hydraul. Res.* 46(3): 356-375.
- Zeng, J., Contantinescu, G., Blanckaert, G., and Weber, L. (2008). "Flow and bathymetry in sharp open-channel bends: Experiments and predictions." *Water Res. Research* 44, W09401.

Appendix

This appendix details the work contracted to Colorado State University Engineering Research Center by the United States Bureau of Reclamation, and the deliverable items which fulfill contractual obligations.

Table 7A. Summary of contractual items and deliverables

Mod. No.	Mod. start date	Mod. end date	Service (task) No.	USBR task No.	Service title	Description	Pertaining documents	Deliver-ables	Summary of deliverables
Mod. 1	9/30/07	9/30/08	1	6	Testing of additional spur-dike design with native topography configurations	No deliverables specified. Completed test matrix and data report.	Scurlock et al. (2012b)	Youngblood et al. (2011)	Youngblood et al. (2011) summarized testing of spur-dikes in the native-topography. Structure design, data collection schemes, and collected velocity and boundary shear-stress data are detailed.

Mod. No.	Mod. start date	Mod. end date	Service (task) No.	USBR task No.	Service title	Description	Pertaining documents	Deliver-ables	Summary of deliverables
Mod. 1	12/1/08	6/1/08	2	7	Evaluation of shear stress in channels - provide guidance for the appropriate shear stress computations	Final to AAO and Drew(6-30-2012)	Ursic (2011), Scurlock et al. (2012d)	Sin (2010)	Sin (2010) investigated methods of shear-stress determination in the trapezoidal physical model
Mod. 2	9/3/09	9/3/10	1	8	Development of design guideline for determining max shear stress from native bed data	Final to AAO and Drew(6-30-2012)	Sin (2010), Scurlock et al. (2012d)	Ursic (2011)	Ursic (2011) investigated methods of shear-stress determination in the native-topography physical model
Mod. 2	9/3/09	11/3/09	3	10	Statistical analysis of interim transverse instream structure design equations	Being re-calculated by include latest structure types	Heintz (2002), Darrow (2004), Schmidt (2005), Scurlock et al. (2012b)	Scurlock et al. (2012a)	Scurlock et al. (2012a) developed empirical design equations for the evaluation of <i>MVR</i> at the outer-bank of the trapezoidal model.

Mod. No.	Mod. start date	Mod. end date	Service (task) No.	USBR task No.	Service title	Description	Pertaining documents	Deliver-ables	Summary of deliverables
-	-	-	-	-	Native topography baseline data	Part of previous work not included in this list of modifications. Report documenting baseline data for two different downstream boundary conditions	Heintz (2002), Walker (2009)	Scurlock et al. (2012c)	Draw-down, and normal-depth boundary conditions were evaluated in the native-topography model. Data are presented and trends were discussed.

Mod. No.	Mod. start date	Mod. end date	Service (task) No.	USBR task No.	Service title	Description	Pertaining documents	Deliver-ables	Summary of deliverables
Mod. 3	12/1/10	12/1/11	1	14	Completion of Native Bed Topography Dataset Evaluation	Summary of performed data collection and analyses	Heintz (2002), Darrow (2004), Schmidt (2005), Walker (2009), Sin (2010), Ursic (2011), Youngblood et al. (2011), Scurlock et al. (2012a), Scurlock et al. (2012b), Scurlock et al. (2012c), Scurlock et al. (2012d)	Current paper	Velocity trends between the trapezoidal and native-topography physical models are depicted and analyzed.

Mod. No.	Mod. start date	Mod. end date	Service (task) No.	USBR task No.	Service title	Description	Pertaining documents	Deliver-ables	Summary of deliverables
Mod. 3	12/1/10	12/1/11	2	15	Development of revised velocity equations for transverse instream structures in the trapezoidal model	Re-write to include all new equations. Draft report completed and in review - lacking step-by step design procedure and recommended limitations of equations. Step by step procedure was included in several other past reports but will be included in this report with the updated equations.	Heintz (2002), Darrow (2004), Schmidt (2005), Scurlock et al. (2012a)	Scurlock et al. (2012b)	Trapezoidal equations expanded to include a variety of transverse instream structure types. Design equations were developed with limitations discussed.

Mod. No.	Mod. start date	Mod. end date	Service (task) No.	USBR task No.	Service title	Description	Pertaining documents	Deliver-ables	Summary of deliverables
Mod. 3	12/1/10	12/1/11	3	16	Development of procedures to estimate longitudinal shear stress distribution on the outside of a bend	Currently conducting data analysis. Report in progress ?	Sin (2010), Ursic (2011)	Scurlock et al. (2012d)	A comprehensive literature review of channel-bend shear-stress distributions was conducted, and trapezoidal and native-topography shear-stress distributions were compiled.
Mod. 3	12/1/10	8/23/12	4	17	Comparison of Equations developed in Service Two to Field Data Collected by Reclamation	Hec-Ras results have been received from AAO	Scurlock et al. (2012c)	Cox et al. (2012)	<i>MVR</i> and <i>AVR</i> equations of Scurlock et al. (2012b) were applied to Bernalillo, NM field site. Recommendations for field application were made.